energies

MDPI

Review

The Carbon Footprint of Hydrogen Produced with State-of-the-Art Photovoltaic Electricity Using Life-Cycle Assessment Methodology

Mehrshad Kolahchian Tabrizi, Jacopo Famiglietti, Davide Bonalumi * and Stefano Campanari

Department of Energy, Politecnico di Milano, Via Lambruschini 4, 20156 Milano, Italy; mehrshad.kolahchian@polimi.it (M.K.T.); jacopo.famiglietti@polimi.it (J.F.); stefano.campanari@polimi.it (S.C.)
* Correspondence: davide.bonalumi@polimi.it; Tel.: +39-02-2399-3817

Abstract: The production of hydrogen as both chemical feed and energy carrier using low-carbon technologies is one of the solutions to reach net-zero emissions. This paper, firstly, reviews the publications on the life-cycle assessment of photovoltaic (PV)-based hydrogen production focused on the carbon footprint. Secondly, it updates the global warming potential (GWP) values of this H_2 production process considering the state-of-the-art PV panels for installation in Italy. In the literature, H_2 produced in Europe and the rest of the world results in a mean GWP equal to 4.83 and 3.82 kg CO_2 eq./kg H_2, respectively, in which PV systems contribute the highest share. The average efficiency of PV panels assumed in the literature is lower than the current PV modules. Updating the supply chain, efficiency, and manufacturing energy and material flows of PV modules can decrease the GWP value of the H_2 produced by nearly 60% (1.75 kg CO_2 eq./kg H_2, with use of alkaline electrolyzer) in the Italian context, which can be further reduced with advancements in PV panels or electrolysis efficiency. The study proves that advancement in the PV industry and additional savings in the electrolyzer's electrical demand can further decrease the carbon footprint of PV-based H_2.

Keywords: LCA; hydrogen; photovoltaic; carbon footprint; electrolysis

Citation: Kolahchian Tabrizi, M.; Famiglietti, J.; Bonalumi, D.; Campanari, S. The Carbon Footprint of Hydrogen Produced with State-of-the-Art Photovoltaic Electricity Using Life-Cycle Assessment Methodology. *Energies* **2023**, *16*, 5190. https://doi.org/10.3390/en16135190

Received: 30 April 2023
Revised: 21 June 2023
Accepted: 30 June 2023
Published: 5 July 2023

1. Introduction

Over the last decades, hydrogen has been produced mainly for industrial applications through conventional production processes based on fossil fuels. Global warming, increasing energy demand, and energy storage challenge made hydrogen a potential solution for future energy transition scenarios. Therefore, on the one hand, a significant amount of hydrogen should be produced to satisfy the growing market demand. On the other hand, these production methods should meet economic and environmental needs. According to hydrogen production data available from International Energy Agency (IEA) [1], in 2021, less than 1% of the produced hydrogen can be considered low-carbon. Low-carbon hydrogen refers to the hydrogen obtained through technologies with a low climate profile, specifically, low CO_2 equivalent emissions. Figure 1, based on the IEA predictions, shows the current and future status of hydrogen production from different sources. Around 94 Mt of H_2 was produced in 2021, of which more than 80% has been obtained directly from fossil fuels without the application of carbon capture, utilization, and storage (CCUS). Currently, the chemical sector demands the largest share of hydrogen in the market to produce ammonia (36%) and for hydrocracking and desulfurization of fuels in refineries (42%) [2]. Based on a net-zero emissions (NZE) scenario, it is forecasted that in 2030, hydrogen production will reach up to 180 Mt. Production via the application of electricity (34%), and fossil fuels with CCUS (18%) will be responsible for this increase in supply. The corresponding demand for this increase in the production volume comes from new applications (heavy industry, power generation, and synthesis of H_2-based fuels) [1].

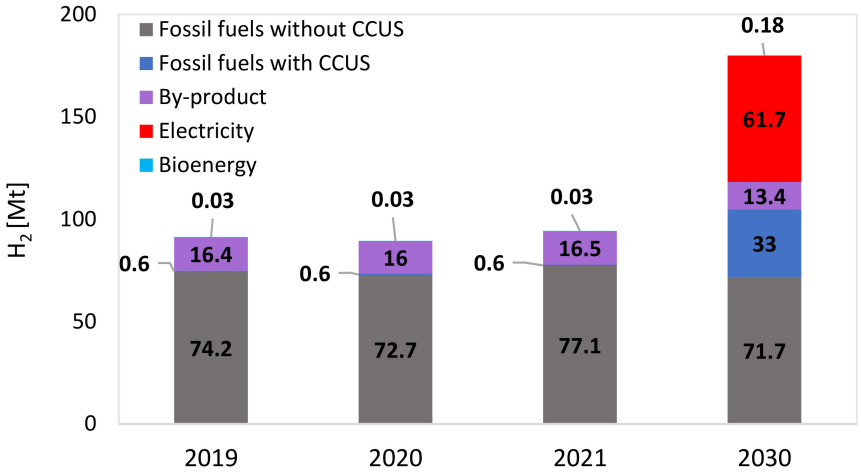

Figure 1. Current and future hydrogen production from different sources (data from [1]).

Hydrogen can be produced using a wide range of processes, including thermochemical, electrochemical, and biological methods. Regarding the diffusion of these processes in new installations, based on the statistical analysis of the available raw data for hydrogen production projects in different stages (operational, under construction, feasibility study, and concept) from IEA [3], more than 80% of new projects are based on electrolysis and less than 10% are powered with natural gas with CCUS. Achieving a low impact from hydrogen production is particularly important in view of its increasing role in the future energy system. For example, the current EU classification for sustainable activities (EU Taxonomy Regulation 2020/852) requires hydrogen production to remain below 3 $kgCO_2$ eq./kg H_2 [4] to comply with a criterion of "substantial contribution to climate change mitigation". Figure 2 shows the number of new hydrogen production projects in Italy and Europe (without Italy). Among the 32 H_2 projects in Italy, 28 of them use electrolyzers. The type of electrolysis system is not disclosed for a considerable number of projects. However, the alkaline electrolyzer has a larger share in Italy for those plants with the known electrolyzer type, followed by proton-exchange membrane (PEM) electrolysis systems. In contrast, in Europe, PEM electrolysis systems are used more frequently.

The electricity powering the electrolyzers to produce H_2 can be supplied from the grid, nuclear, or renewable sources (e.g., wind, photovoltaic, hydro, biomass), usually labeled in the literature as yellow, pink, and green hydrogen. Table 1 introduces the colorful classification of hydrogen production pathways and briefly describes the related process and energy source for each color. The first two lines represent the production processes with high environmental impacts. In contrast, the second group shows the potential of low-impactful production approaches, including the green pathway considered in this work.

Photovoltaic (PV) and wind-based power plants are today the main sources of renewable electricity for new installations. This work focuses on the case of PV electricity and its utilization for green hydrogen production. The environmental impacts of producing H_2 via electrolysis systems powered by renewable electricity have been studied using the process-based life-cycle assessment (LCA) method in several publications (attributional modeling). In 2014, Bhandari et al. [5] reviewed some LCA studies on H_2 production via electrolysis and reported that the global warming potential (GWP) for PV-based hydrogen could vary from 2 to 7 kg CO_2 eq./kg H_2. They mention that higher GWP values for solar PV than hydro or wind are caused by the emissions related to PV module manufacturing processes. In 2018, Parkinson et al. [6] re-estimated the life cycle GHG emissions of a solar PV-based electrolysis system around 2.21 kg CO_2 eq. per each kg of hydrogen. Their calculations assumed a generalized overall energy requirement of 51.2 kWh_{el}/kg H_2 and a 40 g CO_2 eq./kg H_2 for electrolyzer contribution. The related emission of PV systems was estimated based on the review work of Nugent and Sovacool [7]. To the best of the authors' knowledge, the only review paper on PV-based hydrogen was published by Kanz et al. [8],

in which they reviewed and harmonized the GWP values for some related publications up to 2019.

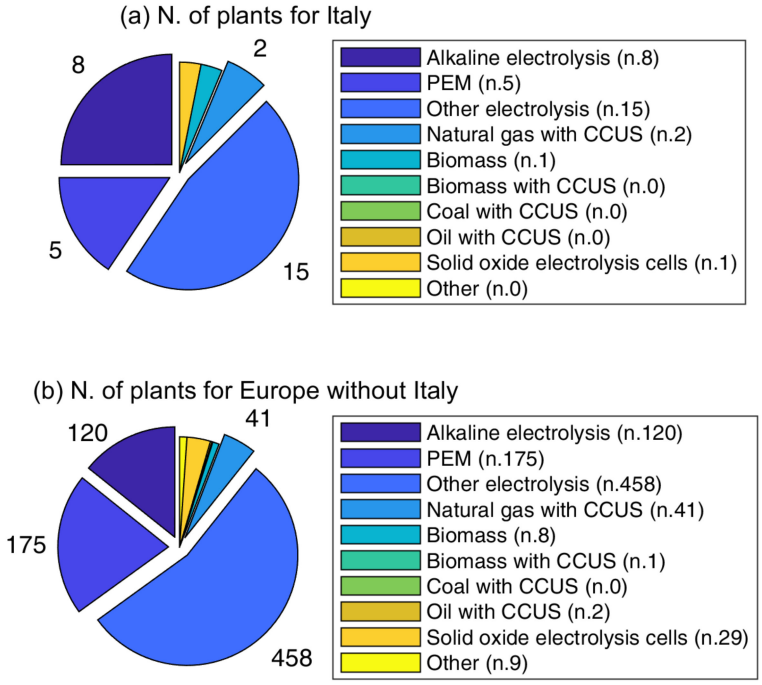

Figure 2. Number of H_2 projects based on different processes for (**a**) Italy and (**b**) Europe without Italy, built based on the raw data from IEA [3].

Table 1. Color classification of hydrogen production pathways.

Category	Color	Process	Source
High environmental footprint (high carbon)	**Brown/Black**	Gasification	Fossil fuels Coal
	Grey	Steam reforming	Fossil fuels Natural gas
Low environmental footprint (low carbon)	**Blue**	Steam reforming or gasification + CO_2 capture and sequestration (CCS)	Fossil fuels Natural gas
	Turquoise	Pyrolysis	Fossil fuels Natural gas
	Yellow	Electrolysis	Water and electricity from the grid (generic)
	Pink/Red	Electrolysis	Water and electricity from nuclear source
	Green	Electrolysis (+biomass *)	Water and electricity from renewable sources/biomass *

* Classification not consolidated.

This paper reviews the literature on the LCA of PV-based H_2 production, more specifically focusing on the GWP impact or the so-called carbon footprint. Moreover, it analyzes the corresponding GWP values of H_2 production using state-of-the-art PV modules. The latest ecoinvent Life Cycle Inventory (LCI) database (version 3.9.1) [9,10] relies on outdated data for PV systems which cannot correctly represent the environmental footprint of the current or near future PV-based installations. Regarding the electrolysis system, the related materials available in ecoinvent to build up the alkaline electrolyzer can still be considered sufficiently updated. However, research and development (R&D) is also positively affecting electrolysis technology in terms of compactness and performance. Therefore, the current paper aims to provide updated GWP values of PV-based H_2 production considering the

current supply chain and state-of-the-art PV panels. The following Sections 2.1 and 2.2 describe different H_2 electrolysis technologies and crystalline silicon PV panel production. The LCA methodology and scenarios are defined in Section 2.3, and the solar PV module supply chain is explained in Section 2.4. The results of the literature review are presented in Section 3. Sections 4.1, 4.2, and 4.3 include the result and discussion of the GWP values in the baseline scenario, the updated PV supply chain, and the carbon footprint of H_2 production, respectively, using the state-of-the-art PV panels for an Italian case study. Finally, Section 5 concludes the paper.

2. Materials and Methods

In this section, the methodology adopted to implement the research is described, providing: (i) a description of the different hydrogen production technologies via water electrolysis, (ii) the electricity source (i.e., photovoltaic), and (iii) the process-based life-cycle assessment method. The articles selected for the literature review are identified using the Scopus database by searching the words "hydrogen" and "life cycle". The search result is refined by the words "photovoltaic (PV)" and "electrolysis". Since the present paper aims to review and analyze the impact of PV panels on hydrogen produced via electrolysis, only the publications reporting at least the carbon footprint of this specific hydrogen production approach are included. In other words, the literature in which extracting the GWP impact of PV-based H_2 via electrolysis is not possible is excluded.

2.1. Hydrogen Production

The water electrolysis process to produce hydrogen and oxygen has been known for two centuries, with the advantage of producing extremely pure hydrogen and a relatively straightforward process based on electricity consumption as energy input. Most applications have been limited to small-scale and unique situations in which access to large-scale fossil fuel-based hydrogen production plants—which dominate today's production, as reported in Figure 1—was not possible or not justified (e.g., electronic industry, food industries as well as medical applications) [11]. Recent developments towards a lower cost of electrolyzers and the perspective availability of low-cost renewable electricity are making their application more attractive. The electrolysis processes can be grouped based on the electrolyte, which may feature different pH (alkaline and acid) or physical state (liquid or solid) [12]. In the following, the 4 most common types of electrolyzers proposed for hydrogen production are shortly explained.

- Alkaline

Among hydrogen production technologies, alkaline water electrolysis is a mature process [13]. Troostwijk developed the first design of an alkaline electrolyzer in 1789 [14], and the technology has followed a long trajectory of research and development, today showing the lowest plant-specific cost (€/kW) with respect to the other types [15]. An aqueous potassium hydroxide (KOH) solution with typical concentrations of 20–40% KOH is used as an electrolyte in alkaline water electrolysis [11]. The cathode and anode electrodes usually are based on low-cost materials (iron or nickel). The alkaline electrolyzer operates between temperatures from 25 °C to 100 °C with 1 to 30 bar of pressure [16]. Formerly, asbestos has been applied as the diaphragm material to avoid mixing hydrogen and oxygen. After the ban on asbestos products [17], other materials such as Zirfon [18] have been introduced. Zirfon is a trademark name for a 500 µm thick, porous material built of 85 wt% ZrO_2 as an inorganic hydrophilic filler bound in a matrix of 15 wt% polysulfone (PSU) [19]. The mature and low-cost alkaline electrolyzers show higher lifetime and production capacity. However, this electrolysis system is mostly designed for a continuous power supply and limited turndown capacity to avoid damage and safe operation [20]. Corrosive environment conditions, risks of leakage of liquid electrolytes, gas permeability, and low current density, bringing to relatively heavy and high-footprint installations, are other disadvantages of this system.

- Proton-exchange membrane

A newer generation of electrolyzers with respect to alkaline electrolysis systems is known as proton-exchange membrane (PEM) electrolyzers. PEM electrolyzers use a thin solid polymer electrolyte (membrane) instead of a liquid electrolyte. Commercial systems use Nafion® as the proton-conducting membrane with a typical thickness of 60–200 µm [21]. Nafion is prepared as a copolymer from tetrafluoroethylene (TFE) and fluorinated vinyl ether, e.g., perfluoro (4-methyl-3,6-dioxane-7-octene-1-sulfonyl fluoride) [19]. The primary advantage of using solid polymer electrolytes is eliminating the need for a circulating aqueous electrolyte and resistances associated with gas bubbles [19]. PEM electrolyzers operate at 50 to 80 °C under pressures up to 70 bar [22]. Typically, platinum-based and iridium-based catalysts are used at the cathode and anode [23], while titanium-based alloys are used for the electrode support and separator plates. Indeed, under the low pH and high electrical potential of PEM operating conditions, titanium is one of the few materials suitable to use on the anode side due to the formation of highly stable thin, compact oxide layers [24]. Compact design, high current density, faster response to load variation, wide turndown capacity, and dynamic operation are obtained by the use of a solid membrane [25]. PEM electrolyzers' other advantages are the possibility of producing highly compressed and pure hydrogen and high efficiency [26]. On the downside, the technology relies on expensive noble metals, such as platinum and iridium (PGM) [16]. The application of such noble metals in addition to titanium and the proton-exchange membranes makes the PEM electrolyzers a tendentially more expensive option than conventional alkaline electrolysis systems.

- Solid oxide electrolyzer cells

Solid oxide electrolyzer cells (SOEC) operate in temperatures higher than 500 °C, typically in the range of 600–850 °C [22]. They can produce hydrogen with a lower electricity input than alkaline and PEM electrolyzers. At the same time, industrial waste heat can be utilized to provide the thermal energy demand of the high-temperature SOEC electrolysis. A SOEC consists of a dense ionic conducting electrolyte and two porous electrodes. Zirconia with different dopants (typically yttria) is the most used material for electrolytes, which allows the conduction of oxygen ions [19]. Alternative materials, especially for low-temperature SOEC, are based on ceria oxides for the electrolyte and the use of metallic supports for the electrodes-electrolyte structure [27]. The cathode is typically made as a heterogeneous structure containing both zirconia and nickel, while for the anode, lanthanum-based perovskites, such as lanthanum strontium cobalt ferrite (LSCF) or lanthanum strontium chromite (LSC) are used [19]. Limited tolerance to thermal cycling and high temperature promoted degradation phenomena of different natures (e.g., delamination of the oxygen electrode from the electrolyte, Cr volatilization from the metal parts, and contamination of the electrodes) are the major problems limiting the lifetime of materials in SOEC, which are still subject of intense R&D and currently at a lower technology readiness level than low-temperature electrolysis [28]. However, SOEC electrolysis systems offer significantly higher efficiency and may achieve a lower total cost of hydrogen production compared to conventional low-temperature electrolysis, thanks to favorable thermodynamics [29]. Additional opportunities are given by the possible simultaneous electrolysis of CO_2 and H_2O for the production of synthesis gas and the possibility of reversible operation as a fuel cell (particularly interesting for energy storage applications) [28].

- Anion-exchange membrane

An anion-exchange membrane (AEM) is an alkaline solid polymeric membrane, which is the core component of an AEM electrolyzer [16]. Applying AEM instead of the conventional diaphragms used in alkaline electrolyzers is the main difference between these technologies [30]. AEM electrolyzers work with an alkaline environment at the membrane interface provided by the immobilized positively charged functional groups on the polymer backbone or pendant polymeric side chains [31]. Trialkyl quaternary ammonium salts

attached to polymeric backbones like polystyrene, polysulfone, poly(ether sulfone), or poly(phenylene oxide) by benzylic methylene groups are most often the anion-exchange group [31]. This type of electrolyzer operates in a temperature range from 40 to 60 °C and under pressures up to 35 bar [22]. A dilute alkaline electrolyte (KOH) is used on the anode side, while no solution is supplied for the cathode side [16]. One of the advantages of AEM electrolysis is its overall lower cost due to the application of transition metal catalyst and the quaternary ammonium ion-exchange-group-containing membrane instead of more expensive noble metal (PGM) catalysts and the Nafion-based membranes [30]. Also, applying a low-concentration alkaline solution as an electrolyte instead of concentrated KOH (without a corrosive liquid) results in the absence of leaking, volumetric stability, ease of handling, and a reduction in the size and weight of the electrolyzer [30]. Catalyst performance deterioration may occur due to the intermittent nature of solar and wind power supplies in the AEM electrolysis. AEMs are susceptible to damage if frequent shutdowns occur on the electrolyzer. Therefore, the durability and conductivity stability of the AEMs should be reinforced considering the large-scale applications and real-world size and conditions within the desired life duration [32].

2.2. Electricity Source—Photovoltaic

Utility-scale photovoltaic (PV) plants include modules, mounting systems, inverters, transformers, cables, electrical protection systems, measurement equipment, and system monitoring [33]. The PV modules produce direct current electricity using solar irradiance and then convert it into alternating current in an inverter for further applications. Crystalline silicon PV panels production starts with silica mining, carbothermic/quartz reduction (removing oxygen from silica), metallurgical-grade silicon (MG-Si) purification, solar-grade (SOG) silicon construction, silicon ingot crystallization, wafer slicing, PV module assembly and finishes with module and laminate construction [34]. The silicon ore is reduced to metallurgical-grade silicon with silicon purity of around 99% via the use of carbon in a large arc furnace [35]. Metallurgical-grade silicon is further refined to 99.999% purity using the modified Siemens process, which is more advanced and less energy-consuming than the original Siemens process [36]. To produce high-purity silicon, the modified Siemens process consumes a considerable amount of energy due to the operation of the reaction chamber at a high working temperature (typically between 1100 °C and 1200 °C) [37], while over the last decade, the energy and material efficiency of the Siemens process has improved remarkably [38]. Single-crystalline and multi-crystalline silicon ingots are obtained by crystallization through the Czochralski process and casting of solar-grade silicon, respectively. These ingots are sliced using a multi-wire saw combined with a slurry of cooling liquid and abrasive particles and then treated by subsequent etching with sodium hydroxide (NaOH) and washing with water and sulfuric acid (H_2SO_4) [36]. PV cells are produced via different steps, surface preparation, dopant diffusion, junction formation, and coating, in which some materials like electric pole printing ribbons, nitrogen, oxygen, and argon are used [35]. Finally, solar cells are connected into a string and then encapsulated by two layers of glass and plastics (ethylene-vinyl acetate) to form the PV module [37].

2.3. Life-Cycle Assessment

The process-based life-cycle assessment (LCA) method is considered one of the most analytical methods to evaluate the environmental profile of products (goods and services), such as hydrogen. Since then, numerous directives, communications, and recommendations of the European Commission have been referred to LCA. The LCA is an internationally recognized method according to the principles defined in ISO 14040 and 14044 [39,40].

In this work, the authors implemented an LCA evaluation using attributional modeling [41], with the scope to evaluate the global warming potential (GWP) impact of gaseous H_2 produced via an alkaline electrolysis system in Italian territory (outcomes related to other 15 impact categories are provided in the Supplementary Materials). Italy is one of

the 6 European countries with an annual renewable electricity potential capacity higher than 600 TWh [42]. The outcomes were calculated using SimaPro 9.4 software [43], the ecoinvent 3.5 library cut-off method as the Life Cycle Inventory database [44], and the Environmental Footprint (EF) 3.0 as the characterization method [45]. The environmental burdens of co-production and end-of-life treatment processes were assessed using the partitioning method in compliance with the ecoinvent library. For modeling the end-of-life scenarios, waste producers bear the burden of waste treatment based on the "polluter pays" principle; consumers of recycled products receive them without charge. The Life Cycle Inventory data (LCI) or foreground data for the alkaline electrolysis system are based on Sundin [46], which relies on Koj et al. [18].

The functional unit is defined as the hydrogen weight (1 kg) following the proposed harmonized life-cycle global warming impact of renewable hydrogen [47]. The boundary system is cradle-to-gate (CTG), in which only the life cycle of hydrogen is considered up to its production. Figure 3 shows the schematic boundary system of this study.

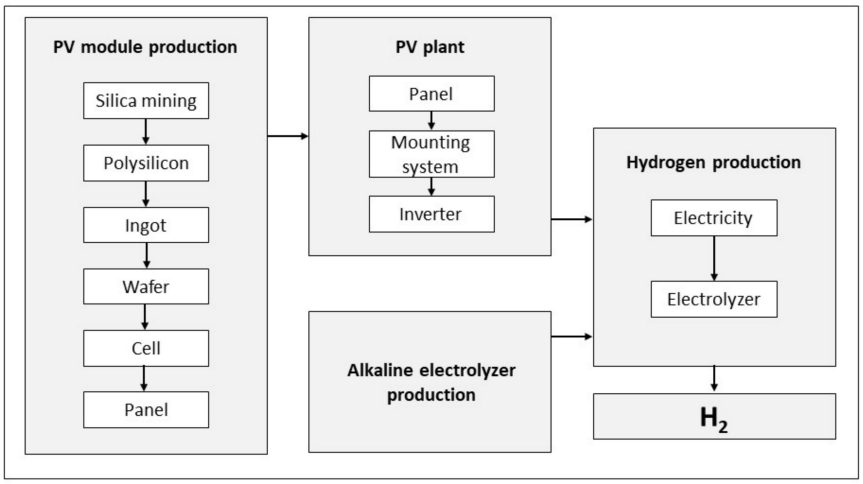

Figure 3. H_2 production schematic boundary system.

Two scenarios have been defined: baseline and updated PV systems.

- For the baseline scenario, the electrolysis system is powered by Italy's default ground-mounted PV system in the ecoinvent database. The ground-mounted PV system in ecoinvent is equipped with multi-Si panels. To make a comparison, the panel is substituted with the available single-Si module in ecoinvent. Consequently, the relative factors, like the area of the PV panels and the mounting system, are adjusted. Also, a sensitivity analysis was carried out, evaluating the impact of: (i) the PV system lifetime, (ii) electrolyzer operating hours in its lifecycle, (iii) the specific electricity consumption of the electrolyzer, and (iv) the solar irradiance (insolation) for the PV plant equipped with ecoinvent default multi-Si panels. The baseline scenario assumptions and limits of sensitivity analysis are summarized in Table 2.
- In the updated scenario, the market supply chain and the main parameters in LCI of PV modules are based on the International Energy Agency special report on solar PV global supply chains and the Task 12 PV sustainability LCI report, respectively [38,48].

The Life Cycle Inventories (LCIs) implemented to model the PV systems are provided in the Supplementary Materials.

The default PV systems considered in the ecoinvent database do not represent current or near-future PV system installations. On the one hand, both the module technology (type and efficiency) and PV panel production processes have evolved. On the other hand, the relative supply chain of PV panels has changed. For example, the single-Si and multi-Si modules in the ecoinvent have efficiencies equal to 14 and 13%, respectively, while the available panels in the current market can offer efficiencies of up to 22.4% [49]. The total

weighted efficiency of crystalline silicon wafer-based modules regarding the total shipment in 2020 is 20.4% [49]. Over the last decade up to 2018, the multi-Si modules had a higher share in the market. In the last few years, single-Si panels become the dominantly produced modules with more than 90% of cumulative global production [38].

Table 2. Description of electrolyzer and PV system in the baseline scenario and sensitivity analysis limits.

Parameter	Description	Sensitivity Analysis Limits
Location (Insolation [kWh/m^2 year])	Italy (1250)	1250–2200
PV system lifetime [years]	30	15–30
Annual specific yield [kWh/kW$_p$]	1033	
Module types	Single-Si, Multi-Si	
Module efficiencies	14%, 13%	
PV system installation	Ground-mounted *	
Electrolyzer type	Alkaline	
Electrolyzer lifetime [hours]	80,000	30,000–80,000
Electrolyzer capacity [MW]	6	
Electrolyzer specific consumption [kWh$_{el}$/kg H$_2$]	50	50–65

* The ground-mounted PV system available in ecoinvent has a capacity equal to 570 kW$_p$. Based on the electricity demand volume, SimaPro software considers a linear relationship and satisfies the demand. In practice, the solar PV plant capacity should be designed to be 3 to 4 times higher than the electrolyzer capacity to satisfy the demand.

Both single- and multi-Si panels with higher efficiencies are considered in the updated scenario. The annual specific yield of PV systems, which defines the amount of electricity produced for each kW$_p$ of PV module over a year, is updated for Italy according to Frischknecht et a. [48]. Also, in order to have a more realistic approach, the annual specific yield is calculated based on the real net PV electricity production data. Values were collected from Terna—the Italian electricity transmission operator [50]. The annual specific yield is estimated based on the published data for installed capacity and net production of PV systems over the three-year period of 2019–2021. This value is calculated for Italy and the three regions of Lombardy, Lazio, and Sicily as representative of the country's north, center, and south, respectively. The related values used in the updated scenario are reported in Table 3. The assumptions corresponding to the electrolyzer remain unchanged.

Table 3. PV system assumptions for the updated scenario.

Parameter	Description
PV system lifetime [years]	30
Annual specific yield—Italy [kWh/kW$_p$]	1376 [48]
Annual specific yield—Terna, Italy [kWh/kW$_p$]	1114
Annual specific yield—Terna, Lombardy [kWh/kW$_p$]	952
Annual specific yield—Terna, Lazio [kWh/kW$_p$]	1189
Annual specific yield—Terna, Sicily [kWh/kW$_p$]	1242
Module types	Single-Si, Multi-Si
Module efficiency	20% [51], 18% [48]
PV system installation	Ground-mounted

2.4. Photovoltaic Module Supply Chain

The supply chain of products can play an important role in their LCA analysis. The effect of the supply chain on the final impact becomes more significant for products with high manufacturing energy consumption, such as PV modules. Considering the supply chain for the different stages of solar PV manufacturing, China dominates the market and then the Asia-Pacific region countries (APAC), as is evident in Figure 4, in red and yellow colors, respectively. According to IEA [38], China is responsible for almost 80% and 97%

of solar-grade polysilicon and wafer production in 2021. Similarly, 85% and 75% of cells and modules were produced in China. APAC countries are the second largest cell and module producers, with around 12% and 15% share in the market. While the ecoinvent database still relies on outdated supply chain data, in which the share of Asia is less than 50% (China is less than 25%) in all stages of PV panel production. Correspondingly, a higher production share is assigned to Europe and North America in ecoinvent. On the demand side, China still is the biggest PV module consumer, while Europe, North America, and APAC countries rank as the second, third, and fourth PV panel end users (almost 18, 17, and 13% of the market, respectively).

As it was stated before, Italy is the selected location for this study and the market analysis should have been carried out for this region; however, the publicly available data for the PV market consider Europe as a whole. Therefore, a similar trend is assumed in the European and Italian markets. Based on the cumulative international shipments of cells and modules for the period of 2017–2021 available in [38], Europe imported 40% and 26% of its cell and panel demands from APAC countries. However, based on only the 2021 data, the cell and module production in APAC countries is almost equal to their demand. Also, considering the U.S. trade restriction on the Chinese module [38], it is decided to satisfy European cell and panel demand with Chinese production. This assumption results in a more conservative LCA analysis due to the higher share of coal-based electricity in China (higher electricity carbon intensity) compared to APAC countries.

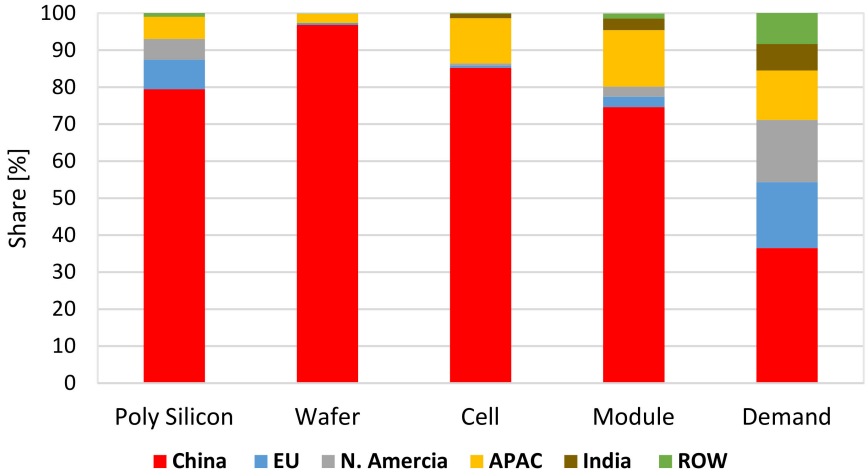

Figure 4. Solar PV production by country and region, 2021; the plot is based on [52].

3. Literature Review Results and Discussion

This section lists and discusses previous works on the topic, providing (i) background and foreground data used, (ii) photovoltaic module efficiency and typologies, and (iii) statistical analysis of the outcomes.

3.1. Literature Review

Regarding the search words, almost 150 articles are found. The articles that do not provide the possibility to extract the GWP impact of H_2 produced via PV-powered electrolysis are excluded. For example, in some articles, a hybrid electricity source is considered; therefore, these publications are out of the scope of this work. Comparing the articles found in the search campaign and the review work of Kanz et al. [8], in which only 13 works were found for the review, a total number of 22 publications (21 peer-reviewed and 1 book chapter) on the LCA of PV-based H_2 are identified. Based on the year of publication, the details of these studies are reported in Table 4. In the following, a brief description of each publication is presented. Sections 3.2 and 3.3 summarize the LCA data sources and PV modules (types and efficiency). The GWP values from the literature are discussed in Section 3.4.

In 2004, Koroneos et al. [53] estimated a value of around 6.2 kg CO_2 eq. per each kg of liquefied hydrogen produced from PV-based electrolysis. Their comparative assessment of the various H_2 production methods was based on the Global Emission Model for Integrated Systems (GEMIS) database [54]. They reported that PV-based hydrogen shows the worst environmental performance compared to other production routes due to the high contribution of the PV module manufacturing process. The paper does not provide enough information on related assumptions like the size of the PV system, the capacity of the electrolyzer, etc. It can be guessed that the location of the PV system was considered to be in Germany due to the use of a German database.

In 2006 and 2007, Granovskii et al. [55,56] performed an LCA of hydrogen produced from both renewables and natural gas using an exergetic approach. The difference between the greenhouse gas (GHG) emissions of the solar-based H_2 in their two articles comes from the different assumptions on the compression stage. In fact, the produced hydrogen before compression results in a GWP value equal to 2.1 kg CO_2 eq./kg H_2 (65% comes from the PV system). The data for the PV system was adopted from a study for building integrated thin-film amorphous silicon panels in Colorado [57]. They did not reveal the type of electrolyzer, but it can be guessed that an alkaline electrolysis system was used. Their electrolysis system is based on the work of Mann and Spath [58], who used an electrolyzer with a Ryton membrane, which is typical for an alkaline electrolysis system.

Simons and Bauer [59] conducted an LCA analysis for different H_2 production processes using the ecoinvent database and published their work in a book chapter in 2011. The data for the electrolyzer's specific consumption and capacity is based on Ivy [60], while the PV system is the default of ecoinvent [61]. The PV electricity assumed by Simons and Bauer is the production mix of Spain, including rooftop and façade installations. They calculated a 4.4 kg CO_2 eq./kg H_2 as the related GHG value for the production and compression of hydrogen up to 45 MPa. In the same year, Lombardi et al. [62] calculated the impacts of H_2 produced based on three different approaches, including the PV system, using some primary data from Italy. They reported a GWP value equal to 6.4 kg CO_2 eq./kg H_2. In 2012, Cetinkaya et al. [63] performed an LCA analysis of various hydrogen production methods. Their assumptions and references for PV-based hydrogen are similar to the previous articles of one of the authors [55,56]. The main difference is the location, which is substituted with Ontario, Canada. They reported a slightly higher GWP value (2.41 kg CO_2 eq./kg H_2) compared to their previous work, probably due to lower irradiations in Ontario (Canada) than in Colorado (USA). Manufacturing of PV modules is responsible for 63% of the overall GWP impact, while the electrolyzer causes no impact.

In 2013, Pereira and Coelho [64] performed an LCA of hydrogen for fuel cell vehicles (FCV) in Portugal. They found a GHG emission equal to 6.35 kg CO_2 eq./kg H_2 for gaseous hydrogen produced via PV-powered electrolysis using the GREET [65] and GEMIS models. The PV system is responsible for 56% of this emission. However, no further details on the hydrogen production system are provided within the work. In 2015, Reiter and Lindorfer [66], using GaBi software [67], assessed the GWP of power-to-gas technologies, including H_2 production from PV. Their production system was considered in EU-27 and resulted in a 3.05 kg CO_2 eq./kg H_2 as the GWP value. Later in that year, Suleman et al. [68] calculated the environmental impacts of H_2 produced using different electrolytic cells. They reported a GWP value equal to only 0.37 kg CO_2 eq./kg H_2 for the Na-Cl electrolysis system powered by PV. Life cycle inventory for chemicals from the ecoinvent database [69] was used for the electrolysis systems. These electrolytic cells co-produce chlorine and caustic soda in addition to H_2. Depending on the adopted allocation approach (for example, mass-based), they can result in a very low amount of electricity demand to produce 1 kg of hydrogen. The allocation method is not mentioned in their work, where the very low obtained GWP value can be confusing to the reader.

In 2017, Zhang et al. [70] published an LCA study of power-to-gas technologies, including PV-based H_2, using both alkaline and PEM electrolyzers. The production site was set to Switzerland, and the background data were extracted from ecoinvent 3.1. They

calculated GWP values equal to 5.59 and 4.76 kg CO_2 eq./kg H_2 for alkaline and PEM electrolysis systems, respectively. The slightly better environmental performance of the PEM electrolysis system was obtained due to its higher average efficiency. Ozawa et al. [71] assessed the GHG emission of hydrogen supply chains to be used in FCVs in Japan. One of the renewable H_2 supply chains considers the production of hydrogen via electrolysis powered by Australian solar PV. They used the Japanese Inventory Database for Environmental Analysis (IDEA) [72] as the background library, in which the GHG emission data were modified to present the Australian PV-based H_2 production. Based on the mean value of specific alkaline and PEM electricity consumption from other studies, they calculated a GWP value equal to 4.16 kg CO_2 eq./kg H_2 for renewable hydrogen production (the rest of the supply chain is excluded). The first detailed LCA study on hydrogen production powered by PV was published by Rivera et al. [73] in 2018. They assessed the environmental impacts of a PEM electrolysis system that provides hydrogen as a cooking fuel in developing countries. Their analysis was based on ecoinvent 3.1 and resulted in a GWP equal to 3 kg CO_2 eq./kg H_2. It is reported that 90% of the GWP value is caused by the production of PV panels and their associated components in China. Their PV system includes ground-mounted multi-Si panels with an efficiency of 14.2% in an area with a solar global horizontal irradiance (GHI) equal to 2000 kWh/m^2 per year.

In 2020, Sadeghi et al. [74] conducted an LCA analysis, including a solar PV-based hydrogen production facility to feed refineries or chemical industries. The solar PV system was considered to be located in the Markazi province (Iran), with an insolation of around 2200 kWh/m^2 per year. Their alkaline electrolyzer specifications were based on Koj et al. [13], considering a 3.9 MW capacity. It seems that the corresponding GWP value for each kWh of electricity produced by solar PV is adopted from Miller et al. [75], in which the background data is based on ecoinvent inventory. Sadeghi et al. reported a GWP value equal to 3.08 kg CO_2 eq. per each kg of hydrogen produced via electrolysis, from which 88% is generated from PV module manufacturing and plan construction. Al-Qahtani et al. [76] applied an LCA analysis of different hydrogen production pathways to find out the true cost of hydrogen via life cycle monetization. They considered the United States (US) as the location of their study and used ecoinvent 3.4 as the background data. They declared that the environmental impacts of the electrolyzer were omitted since the main contributor to the total environmental impact is electricity consumption. Considering the effect of consumed PV electricity by a PEM electrolysis system based on Colella et al. [77], a GWP value equal to 3.45 kg CO_2 eq./kg H_2 is reported.

Among the reviewed articles, Palmer et al. [78] presented a detailed LCA analysis in 2021. The PV system includes a lithium-ion battery (LIB) to maintain the minimum electrolyzer operation during periods of low PV electricity. The hydrogen produced under their solar-battery scenario results in 2.3 kg CO_2 eq./kg H_2. The solar PV system, battery, and electrolyzer represent 82%, 10%, and 4% of the GHG emissions, respectively. The PV system is equipped with multi-Si Chinese panels with an efficiency equal to 16.8%. The single-axis solar tracking configuration considered in their work scales up the electricity production by a factor of 1.2 compared to a fixed-tilted plane installation. The PV system is mounted in a location in Australia with a relatively high solar GHI (2200 kWh/m^2 year).

The highest number of related articles (5 of 22) were published in 2022. Hermesmann and Müller [79] gathered the environmental impacts of different hydrogen production approaches based on the available data from literature and the ecoinvent database. They calculated an almost 5 kg CO_2 eq. per each kg of hydrogen produced via solar PV-based PEM electrolysis system in Germany. In contrast to other studies, they assigned environmental credit for the oxygen co-produced via electrolysis using the substitution approach. However, for the PV-based H_2, the breakdown of the results is not presented. Later in that year, Zhang et al. [80] reported the highest-ever GWP value in the related literature, which is equal to 9.37 kg CO_2 eq./kg H_2 for a PEM electrolysis system in Gansu, China (GHI = 1782 kWh/m^2·year); 78% of the GWP impact is generated due to the construction of the solar PV plant and 21% from the construction of the hydrogen plant. Based on (i) the

reported total electricity production of the PV plant, (ii) the annual H_2 output of the PEM electrolyzer, and (iii) their capacities, the relation between the production data and units of the electrolyzer and PV plant does not result in an integer number. Also, it is reported that the whole system's specific consumption is 54.81 kWh_{el}/kg H_2 under the full load operation, while the actual overall specific consumption is 60 kWh_{el}/kg H_2.

Still, in 2022, Kolb et al. [81] performed an LCA analysis for large-scale H_2 production in three different sites for the final user in Germany. They adopted the LCI of the PEM electrolyzer from Bareiß et al. [21] and modified the ecoinvent database to calculate the impact of electricity produced from the PV system. Their study includes the liquefaction and shipping distance impacts on imported hydrogen. They concluded that the import of PV-based hydrogen could environmentally outperform domestic production. The GWP values of only the H_2 production part (liquefaction and transportation excluded) are 2.09, 3.08, and 5.08 kg CO_2 eq./kg H_2 for Chile, Morocco, and Germany. Freire Ordóñez et al. [82] evaluated the economic and environmental aspects of e-fuels. An LCA analysis was carried out for green hydrogen production as input for the chemical plant. Their assessment for large-scale PV and PEM electrolysis systems in the United Kingdom, Germany, France, Spain, and Italy resulted in GWP values equal to almost 4.50, 5.65, 4.70, 3.80, and 4.10 kg CO_2 eq./kg H_2, respectively. They did not consider the environmental impacts of the PEM electrolyzer manufacturing due to their low contribution to the environmental impact of green H_2, where most of the impacts are caused by the used electricity (embodied fossil energy in solar panels in the case of PV systems). Aydin and Dincer [83] performed an LCA analysis of various hydrogen production methods to be used in refueling bus stations in Ontario, Canada. Using the ecoinvent database, the solar-based H_2 production via the PEM electrolysis system resulted in 6.8 kg CO_2 eq./kg H_2 as the GWP impact, which is relatively higher compared to an older publication [63] for PV-based H_2 production in the same region.

Weidner et al. [84] recently assessed the environmental performance of large-scale (500 Mt/year) green and blue hydrogen production using prospective life cycle analysis. It is stated that, in general, the GWP impact generated from green hydrogen comes from the renewable energy infrastructure. Based on the global or Rest of the World (RoW) PV dataset in ecoinvent, they calculated GWP values equal to 3.9, 2.9, and 1.3 kg CO_2 eq./kg H_2 for solar-based PEM electrolysis system in years of 2019, 2035, and 2050, respectively. It is reported that the expected reduction in the carbon footprint of PV-based hydrogen is caused by cleaner electricity production in China compared to the current relatively coal-based power generation. Finally, in the most recent paper, Vilbergsson et al. [85] analyzed the environmental impacts of H_2 production in Austria, Belgium, and Iceland, considering different scenarios. One of the scenarios examines PV-based hydrogen production, assuming intermittent real solar availability (995 h/year) in Belgium using PEM and SOEC electrolyzers. The emission related to PV electricity is extracted from the GaBi database, while the background data for electrolyzers is based on both GaBi and ecoinvent. They reported GWP values equal to 4.60 and 3.02 kg CO_2 eq./kg H_2 for PEM and SOEC electrolysis systems, respectively. Another scenario assumes purchasing a PV certificate to increase the operating hours to 8000 annually. Under this, GWP values decrease to 4.05 and 2.69 kg CO_2 eq./kg H_2. By increasing the operating hours, the share of electricity in the GWP impact increases from nearly 86% to 98%, as the impact of the electrolyzer is mitigated. The lower carbon intensity of the hydrogen produced via SOEC electrolysis is mainly due to the higher efficiency of this type of electrolyzer (lower specific electricity consumption).

Table 4. Summary review of publications.

Paper	Year	Location	PV Capacity [MW]	PV Lifetime [years]	Panel Type	Elec. Type	Elec. Capacity [MW]	Elec. Specific Consumption [$kWh_{el}/kg\ H_2$]	Elec. Lifetime [hrs]-(Years)-[Stack Life Time-Years]	GWP Value [kg CO_2 eq./kg H_2]	Foreground Data	Background Data
Koroneos et al. [53]	2004	Germany [a]	--	--	--	Alk	--	51.17	--	6.2	--	GEMIS
Granovskii et al. [55,56]	2006–2007	Silverthorne, Colorado	0.001231	30	Thin film	Alk	0.135 [b]	49.8	--	2.1	Secondary	N. A.
Simons & Bauer [59]	2011	Spain	--	30	--	Alk	0.25 [c]	47 (57) [d]	--	4.4	Secondary	ecoinvent
Lombardi et al. [62]	2011	Florence, Italy	2.34	20	Multi-Si	Alk	0.584 (0.073 each module)	58.5	87,600 [e] (10 years)	6.4	Primary & Secondary	SimaPro database
Cetinkaya et al. [63]	2012	Toronto, Canada	0.008	30	Thin film	Alk	0.135 [b]	49.8	--	2.41	Secondary	N. A.
Pereira & Coelho [64]	2013	Portugal	--	--	--	--	--	--	--	6.35	--	GEMIS GREET
Reiter & Lindorfer [66]	2015	EU-27	--	--	--	Alk or PEM	--	57.6	--	3.05	Secondary	GaBi
Suleman et al. [68]	2015	Canada [f]	--	--	--	Na-Cl	--	1.3	--	0.37	Secondary	ecoinvent
Zhang et al. [70]	2017	Switzerland	--	30	--	Alk PEM	0.3 0.1	57.9 54.5	67,000	5.59 4.76	Secondary	ecoinvent 3.1
Ozawa et al. [71]	2017	Australia	10	30	--	Alk PEM	--	57.75	--	4.16	Secondary	IDEA
Rivera et al. [73]	2018	Developing countries [g]	0.1008	20	Multi-Si	PEM	0.041 [h]	52.36	(20 years)	3.07	Secondary	ecoinvent 3.1
Sadeghi et al. [74]	2020	Markazi, Iran	118.8 [j]	30	Single-Si	Alk	(3.9 each module)	57.5	(30 years) [15 years]	3.08	Secondary	N. A.
Al-Qahtani et al. [76]	2020	US	0.570	30	Multi-Si	PEM	113 [k]	54.2	[7 years] [k]	3.45	Secondary	ecoinvent 3.4
Palmer et al. [78]	2021	Pilbara, Australia	1010	20	Multi-Si	Alk	550 (3.9 each module)	55	73,000 [l] (20 years) [10 years]	2.3	Secondary	ecoinvent 3.5
Hermesmann and Müller [79]	2022	Germany	0.570	30	Multi-Si	PEM	1	55	160,000 [m] (20 years) [10 years]	5	Secondary	ecoinvent 3.6
Zhang et al. [80]	2022	Gansu, China	10	30	Multi-Si	PEM	5	60	109,500 [n]	9.37	Primary & Secondary	N.A.
Kolb et al. [81]	2022	Atacama, Chile; Fes, Morocco; Bavaria, Germany	100	30	Multi-Si	PEM	83 79 98 (1 each module)	55 [o]	(20 years) [7 years]	2.093 3.076 5.082	Secondary	ecoinvent
Freire Ordóñez et al. [82]	2022	UK Germany France SpainItaly	23,500 20,70020,200 15,100 15,700	--	Multi-Si	PEM	8962.96 [P] 9739.9 9092.45 8371.81 8298.62	56.3	--	4.5 5.65 4.7 3.8 4.1	Secondary	ecoinvent 3.5
Aydin and Dincer [83]	2022	Ontario, Canada	--	--	--	PEM	--	60.50	(20 years)	6.8	Secondary	ecoinvent 3
Weidner et al. [84]	2023	Global or [RoW]	0.570	30	Multi-Si	PEM	(1 each module)	55	--	3.9	Secondary	ecoinvent 3.8
Vilbergsson et al. [85]	2023	Mortsel, Belgium	--	--	--	PEM SOEC	1	56.3 37.7	60,000 20,000	4.60 3.02	Secondary	GaBi ecoinvent 3.6

[a]: based on the German database. [b]: calculated based on 30 Nm^3/h from [58] and the specific consumption. [c]: calculated based on 5.4 kg/h H_2 production and 47 kWh/kg H_2 specific electrolyzer consumption. [d]: including auxiliary services and compression to 45 Mpa. [e]: they assumed 24 h operation per day of the electrolyzer. [f]: not mentioned in the manuscript (considered based on the institution of authors). [g]: locations with an average insolation level of 5.5 $kWh/m^2 \cdot day$ (Indonesia, Philippines, India, Jamaica, Brazil, Mexico, Ghana, Nigeria). [h]: based on a 4-stack electrolyzer from [86]. [j]: we calculated this value based on 16% panel efficiency, 1.6 m^2 as area, and 464,000 modules. [k]: reported from [77]. [l]: we calculated this value considering 10 h of production per day in 20 years (stack lifetime = 10). [m]: they considered an 8000 annual operating hours. [n]: calculated based on 10 h per day and 30 years as lifetime. [o]: based on maximum system efficiency (60%) and LHV. [P]: we calculated the electrolyzer capacities based on the hourly production rates and electricity consumption.

3.2. Background and Foreground Data

Among the 22 studies, 50% used different versions of the ecoinvent as a background database [59,68,70,73,76,78,79,81–84]. In five articles, the background data are not introduced [55,56,63,74,80]. Only one study is based on Gabi [66], while another used both Gabi and ecoinvent [85]. Similarly, one study used the GEMIS database [53], while another one is based on both GEMIS and GREET [64]. Also, only one study used the Japanese IDEA database [71]. Lombardi et al. [62] reported SimaPro as a database, whereas SimaPro is a software. Figure 5a shows the library distribution used.

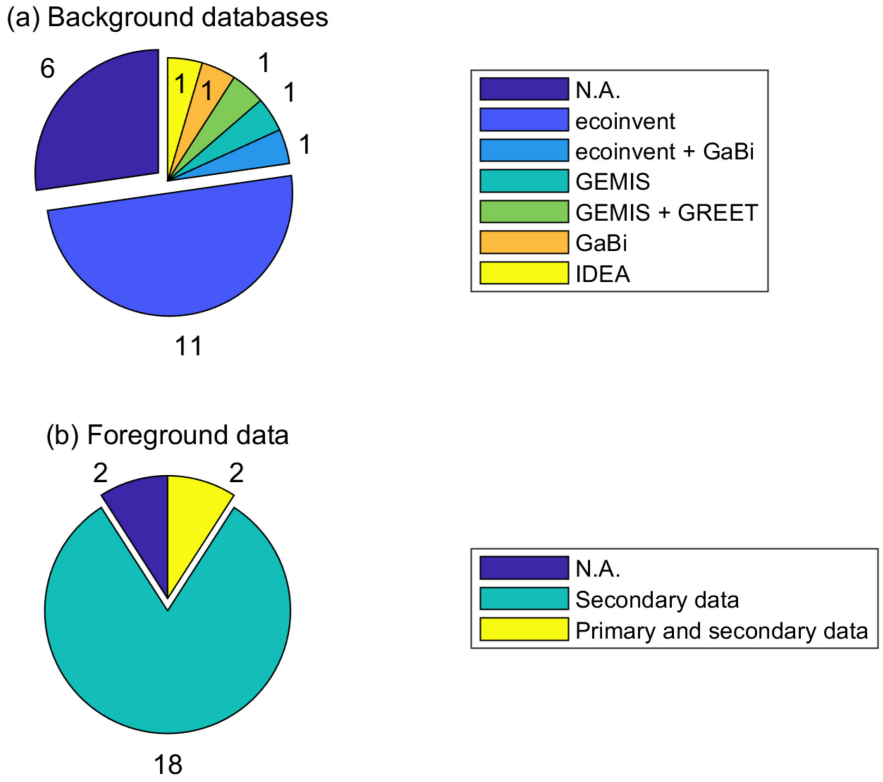

Figure 5. Distribution of (**a**) background databases and (**b**) foreground data.

The Life Cycle Inventory or foreground data can play an important role in LCA. The majority of the reviewed studies (80%) are based on available data from literature or reports (secondary data) [55,56,59,63,66,68,70,71,73,74,76,78,79,81–85]. Only two of the studies reported that partially they had access to some primary data [62,80]. The remaining two studies did not reveal their inventory data [53,64]. The distribution of LCI is indicated in Figure 5b.

3.3. Photovoltaic Module Efficiency and Type

The main component of a solar PV system is the module. Among the reviewed studies, 40% did not mention the solar PV panel type considered in their work [53,59,64,66,68,70,71,83,85]. Multi-Si PV modules are assumed in 9 (40%) of the articles [62,73,76,78–82,84], while only one paper considered single-Si panels [74]. Three of the studies are based on thin-film panels [55,56,63]. The module efficiency is an important factor related to the nominal power of the panel and its area. Higher panel efficiency means a lower area is needed to reach a specific power output.

Some studies did not specify the panel efficiency. In 10 studies, the panel efficiency was reported or it could be realized. Figure 6 shows the trend of PV modules' efficiency (left axis) and the corresponding GWP values for each kg of H_2 (right axis) with respect to the year of the publication. The panel efficiency has increased over time; however, in the case of using the default version of ecoinvent, the increase in efficiency is not applied. The studies [55,56,63] used thin-film PV panels with an efficiency of around 5% according

to the reference they have used, i.e., Meier 2002 [57]. The multi-Si panels considered in [62,73] have an efficiency of 12.7% and 14.2%, respectively. The single-Si modules used by Sadeghi et al. [74] are 16% efficient. The solar PV farm by Palmer et al. [78] is based on multi-Si panels with 16.8% efficiency. Some studies are based on ecoinvent without any further changes for open-ground multi-Si solar plants [76,79,82]. Therefore, they are based on modules with 13% efficiency. The average efficiency of the panels considered in the related literature is only 12.95%. As shown in Figure 6, the GWP value (orange line) does not necessarily decrease with the increase in module efficiency (blue line). Two points can explain this non-trivial behavior. Firstly, the location of the PV site is an important factor in the GWP value of PV-based H_2. For example, the value of 4.6 kg CO_2 eq./kg H_2 shown for multi-Si in 2022 is the average GWP of 6 values for five different locations (Spain = 3.8 kg CO_2 eq./kg H_2 and Germany = 5.65 kg CO_2 eq./kg H_2). Secondly, the quality of the LCA analysis depends on the data quality and transparency, which can significantly affect the climate footprint and lead to inconsistency in the result.

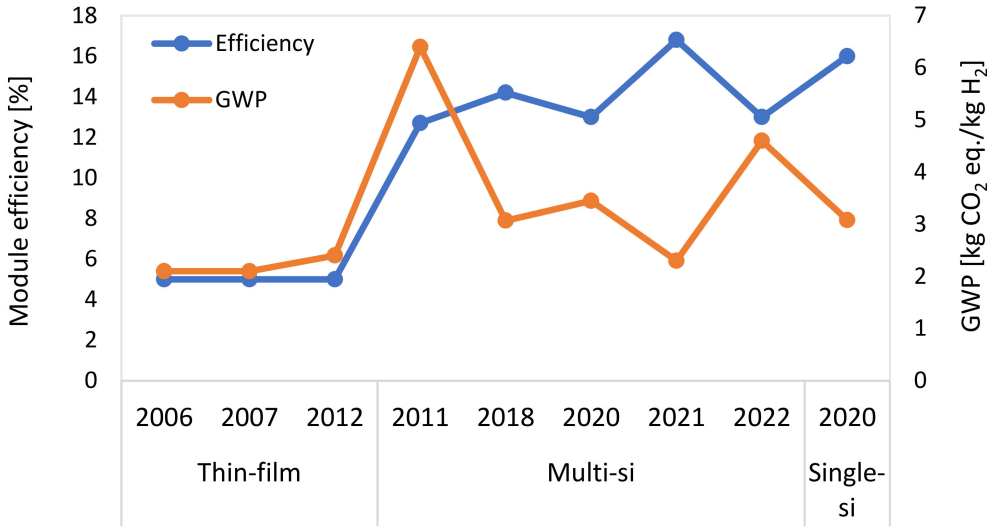

Figure 6. Efficiency and type of the modules and corresponding GWP value of the produced H_2 with respect to the year of publication.

3.4. Statistical Analysis of GWP Values

The GWP values for producing 1 kg of H_2 via electrolysis systems powered by PV, extracted from 21 studies, are divided into two groups: Europe and the rest of the world. Among the 22 studies reviewed, only the work of Suleman et al. [68] is excluded since their GWP value (0.37 kg CO_2 eq./kg H_2) is relatively low and is not comparable with other studies. Their electrolytic cell co-produces chlorine and caustic soda in addition to H_2, resulting in very low GWP values due to: (i) a different electrolysis system compared to the more common alkaline and PEM electrolyzers and (ii) the allocation approach used, which the authors do not specify.

The GWP values are plotted in Figure 7, providing statistical information (i.e., mean, standard deviations, 25th and 75th percentiles). The first column represents 16 GWP values for PV-based H_2 production in Europe. The values fluctuate from 3 to 6.4 kg CO_2 eq./kg H_2, where the mean is 4.83 kg CO_2 eq./kg H_2 with a standard deviation equal to 1.05 kg CO_2 eq./kg H_2. The second column is based on seven studies located outside of Europe (rest of the world), in which exist values as low as 2.1 kg CO_2 eq./kg H_2 and as high as 9.37 kg CO_2 eq./kg H_2. The PV-based H_2 GWP values for the rest of the world show a mean equal to 3.82 with a standard deviation of 2.17 kg CO_2 eq./kg H_2. Comparing the two columns suggests that GWP values for the production of H_2 via electrolysis powered by PV systems in Europe might be higher with respect to production sites outside of this continent. According to the variation of GWP results in the literature, it can be noted that

comparing or interpreting the carbon footprint or, in general, the environmental profile of the PV-based H_2 is not trivial. On the one hand, some works' unclear assumptions or lack of data make comparing the studies even more difficult. On the other hand, different system boundaries and different electrolysis systems can alter environmental footprints. However, this work tried to present the extracted GWP values in a quasi-harmonized manner (in case of possibility compression or liquefaction steps are excluded).

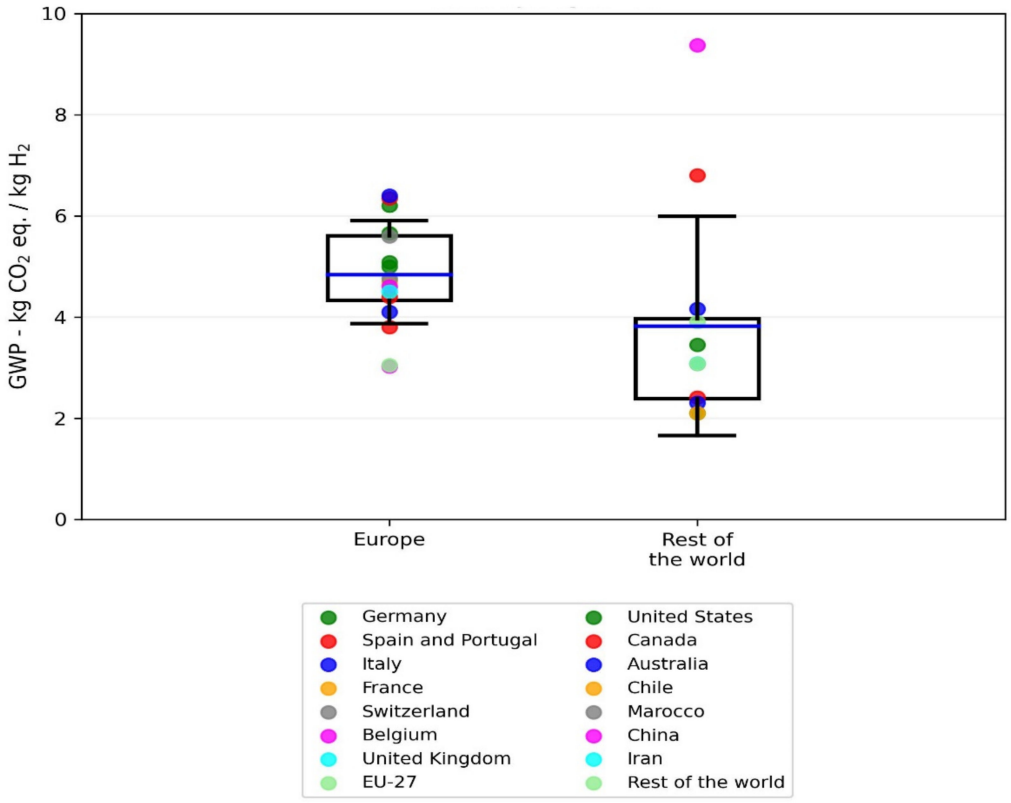

Figure 7. Distribution of GWP values of solar-PV-powered electrolysis system of each kg of H_2 from the literature.

4. Life-Cycle Assessment for Italian Case Study

In this section, the study conducted for the Italian case study is presented, describing: (i) the baseline scenario, (ii) the photovoltaic life-cycle inventory supply chain updated, and (iii) the outcomes achieved.

4.1. Baseline Scenario

The baseline scenario represents the production of H_2 using a 6 MW alkaline electrolyzer powered by the default multi-Si panels and the modified single-Si ground-mounted PV systems for Italy in ecoinvent. This electrolysis system produces 9600 tons H_2 in its lifetime. The GWP values are plotted in Figure 8. These values for each kg of hydrogen produced are equal to 3.78 and 4.28 kg CO_2 eq. for multi-Si and single-Si available PV modules in ecoinvent, respectively. Only less than 2% of the GWP value is generated by the production and operation (use of KOH, etc.) of the alkaline electrolyzer for H_2 production. In comparison, almost the other 98% is caused by the solar PV system. In other words, the key component of the GWP is the production of renewable electricity and not the hydrogen production itself. The significantly higher impact of the PV system on the GWP value is in line with the results of the reviewed literature. The electricity produced using the single-Si modules available in ecoinvent results in 13% higher GHG emission (0.5 kg CO_2 eq.) than the default multi-Si ground-mounted PV system. The main reason behind this worst environmental performance is the higher energy consumption of the

production of the single-Si wafer modules. In other words, the 1% higher efficiency of single-Si panels, which results in lower PV plant area, does not overcompensate for the higher production energy demand. This statement can justify the choice of multi-Si panels for large-scale ground-mounted PV plants in the ecoinvent database.

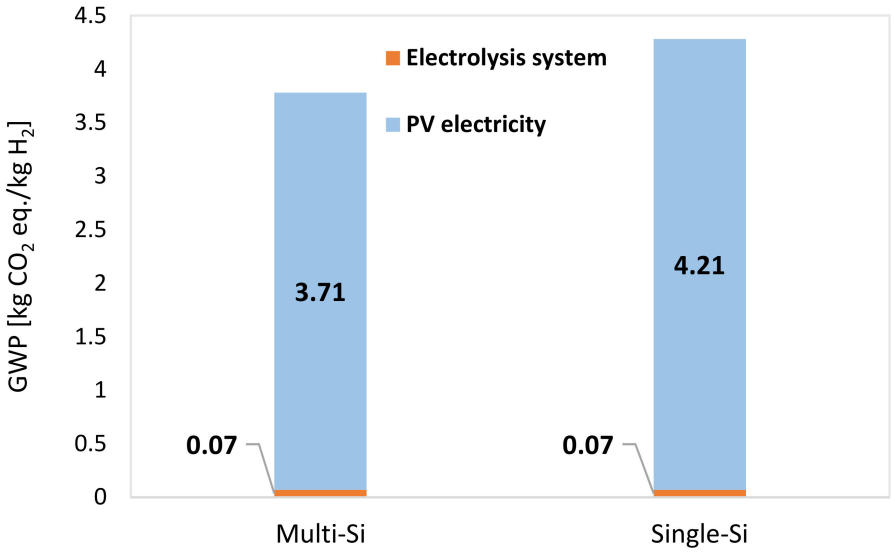

Figure 8. GWP values of each kg of H_2 for the baseline scenario.

A one-at-a-time sensitivity analysis (OAT-SA) was conducted by varying the main factors of solar PV-powered electrolysis systems. The PV plant is equipped with ecoinvent default multi-Si panels. OAT-SA includes the PV system lifetime, electrolyzer operating hours in its lifecycle, the specific electricity consumption of the electrolyzer, and solar irradiance (insolation). Figure 9 shows the GWP behavior of each kg of H_2 produced by the electrolysis system. The variation of factors related to the PV system results in more significant changes in GWP value. PV system lifetime (panels lifetime) and insolation (location of the solar PV site) have higher impacts on the environmental profile of the produced hydrogen. For example, decreasing the PV system lifetime from 30 to 15 years increases the GWP value from 3.78 to 7.36 kg CO_2 eq./kg H_2. The location of the PV site can affect the GWP value remarkably. For places with abundant sunshine (GHI = 2200 kWh/m^2 year), the GWP value can drop around 2 kg CO_2 eq./kg H_2. Increasing the specific electricity consumption of the electrolyzer, the GWP value increase, and vice versa. On the contrary, the variation in the lifetime of the electrolyzer does not cause a noticeable change in the GWP value. The results confirm the smaller share of the electrolyzer production in GWP impact compared to the effect of the PV system, evidencing that the key element in the GWP is the climate profile of electricity production.

From this point of view, further advantages may arise from the implementation of different electrolysis technologies, such as the SOEC, which is expected to require less electricity for the same hydrogen production (e.g., 35–40 kWh/kg H_2 instead of the >50 kWh/kg H_2 assumed for the alkaline electrolysis) [87]. The impact of this option, assuming for simplicity to keep the same carbon footprint for the electrolyzer production and management, would be to decrease the GWP by 20% or more (dashed area in the diagram), depending on the assumptions.

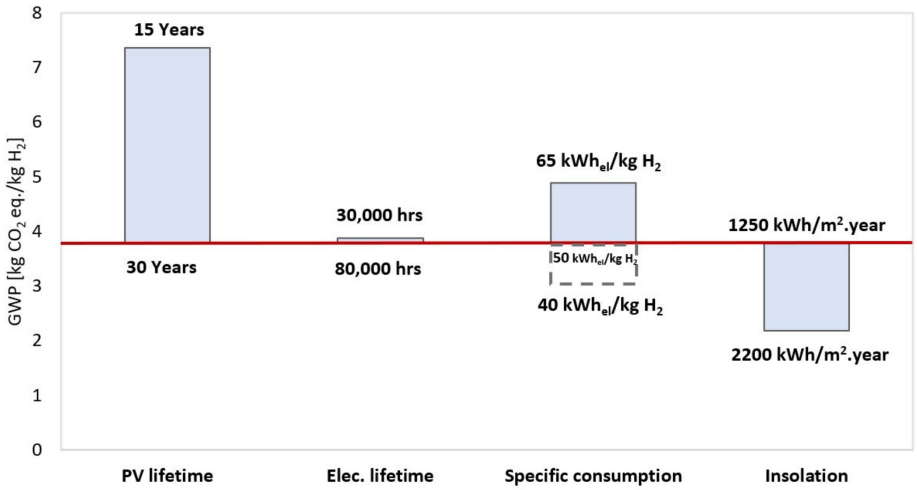

Figure 9. Sensitivity analysis on GWP values of each kg of H_2 for the multi-Si PV system in the baseline scenario.

4.2. Update of the PV Supply Chain

Italy is the selected location for this study, and the market analysis should have been carried out for this region; however, the publicly available data for the PV market consider Europe as a whole. Therefore, a similar trend is assumed in the European and Italian markets. The updated supply chain for PV panels used in Europe during 2021 is shown in Figure 10. Around 32 GW of new PV panels was the European market demand in 2021 [38]. Based on IEA [52] and the assumptions made in Section 2.4, 85% of such panels (27 GW) were manufactured in China, and the rest (5 GW) were European panel productions. Europe produced a 1.1 GW equivalent capacity of PV cells in 2021. The remaining demand for PV cells to produce the 5 GW of modules in Europe was supplied by Chinese cells.

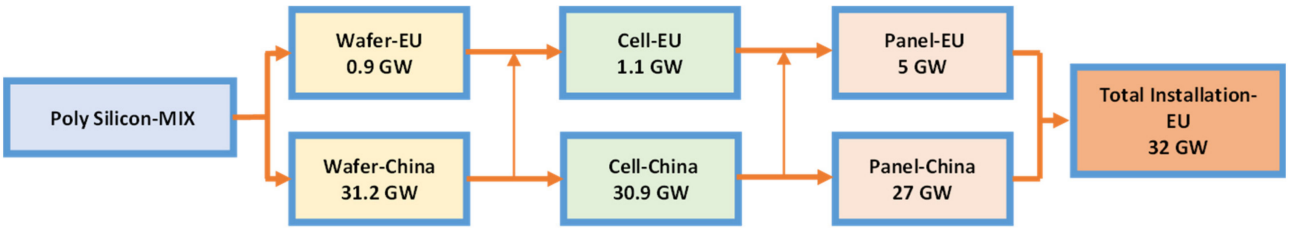

Figure 10. The updated supply chain for PV panels in the European market.

Similarly, 0.9 GW equivalent wafer capacity was produced in Europe, and the rest was imported from China. In other words, of Europe's 32 GW PV market demand capacity in 2021, 97.5% (31.2 GW) is based on Chinese wafer production. The ingot and wafer production stage is the second highest energy consumer after the polysilicon production in single-Si panel manufacturing processes [38]. The polysilicon-mix term in Figure 10 refers to the global market of polysilicon which consists of almost 80% Chinese polysilicon production. Europe, APAC, and North America supply 8, 6, and 5.6% of polysilicon. Solar-grade silicon production is the most energy-intensive production stage [88]. Therefore, China is also responsible for most solar-grade silicon production and its corresponding high-energy consumption and emissions. It can be noted that the solar PV industry of China is located mainly in the provinces of Xinjiang and Jiangsu, where electricity production is heavily coal-based [38].

As stated in Section 2.4, in practice, the share of APAC countries in the European PV market is not negligible. However, in this work, it was preferred to adopt a more conservative approach and neglect APAC-built cells and modules, which are produced using electricity with lower carbon intensity than the Chinese mix. Also, it should be

recalled that Figure 10 presents the assumed supply chain for single-Si PV panels and not for multi-Si panels, which had a very low market share in 2021. However, the supply chain of multi-Si modules is only updated to provide a broader comparison with the baseline scenario. The supply chain considered for multi-Si panels is based only on Chinese PV panel production except for solar-grade silicon (polysilicon), which is similar for both types of PV modules.

4.3. The Carbon Footprint of Hydrogen in the Updated Scenario

The GWP values for hydrogen produced via an electrolysis system powered by state-of-the-art PV panels are plotted in Figure 11. In order to provide a comparison, the GWP values from the baseline scenario are included (the first bar of each type of panel). Similar to the results in Section 4.1, a GWP value equal to 0.07 kg CO_2 eq./kg H_2 is generated from the electrolyzer production and operation, which is embedded in the overall GWP value of all cases. For the updated scenario and each type of PV panel, the second bar represents the modified market supply chain, the efficiency, and the energy and main material flow in the manufacturing of PV panels, besides the annual specific yield according to [48]. The third bars are created on similar assumptions of the second bars except for the annual specific electricity production, which is substituted with the real data from Terna [50]. The updated scenario results in almost a 52% and 59% reduction in GWP values for each kg of H_2 for multi-Si and single-Si modules compared to the baseline scenario (ecoinvent default ground-mounted PV system), respectively. For the multi-Si panels, 3.78 kg CO_2 eq./kg H_2 is reduced to 1.83 kg CO_2 eq./kg H_2, while for the single-Si modules, which is the state-of-the-art PV system technology, a 2.52 kg CO_2 eq./kg H_2 reduction in GWP is obtained. In the case of using real data for PV electricity production in Italy, the GWP values for both types of updated PV modules increase by more than 22% (almost 0.4 kg CO_2 eq./kg H_2), which means that multi-Si and single-Si PV systems result in 2.25 and 2.15 kg CO_2 eq./kg H_2. However, still using the real data and updated scenario offers a CO_2 eq. mitigation equal to 40% and 50% for multi-Si and single-Si ground-mounted PV systems with respect to the baseline scenario.

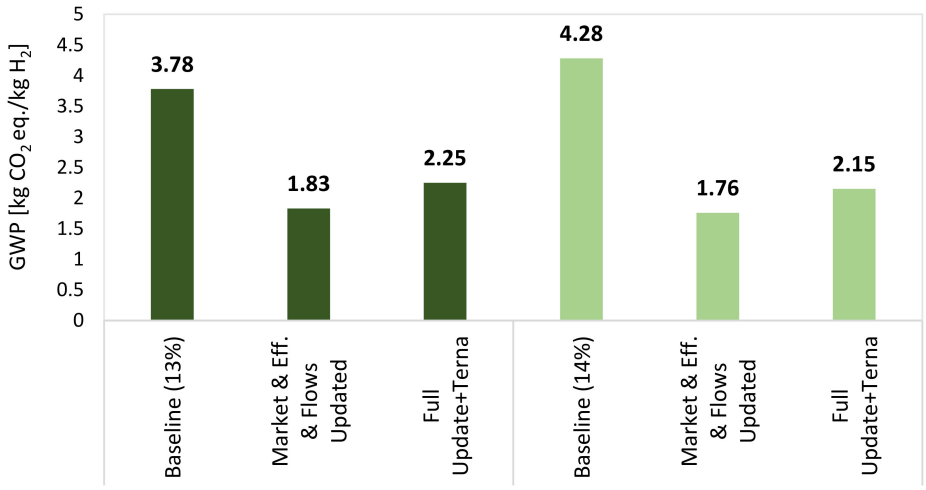

Figure 11. GWP values of each kg of H_2 for the updated scenario.

Under the updated scenario assumptions, comparing the two types of crystalline silicon modules shows an almost 4% lower GWP value obtained for hydrogen produced using single-Si PV systems. As it is stated in Section 4.1, for outdated crystalline silicon panels, multi-Si PV systems environmentally outperformed single-Si panels by a 13% lower GWP value. Both the advancement in the efficiency and the more efficient production processes of state-of-the-art single-Si modules led to lower GWP values of the electricity produced and, consequently, greener hydrogen. The difference in the efficiency of outdated single-Si and multi-Si modules is only 1%, while this value for the state-of-the-art crystalline

silicon panels is at least around 2%. This cell technology can offer even higher efficiencies despite the higher energy demand of single-Si wafer production. For example, if the efficiency of the single-Si module increases from 20% to 22% (the best single-Si lab module offers efficiencies up to 24.4% [49]), the GWP value of each kg of H_2 can decrease to 1.61 kg CO_2 eq. (1.98 kg CO_2 eq./kg H_2 for the real PV annual specific yield data from Terna). Similarly, if the panel efficiency increases up to 25%, the GWP value will further drop to 1.44 kg CO_2 eq./kg H_2. On one side, for the 22% efficient panel, the 2% increase in module efficiency translates to an 8% decrease in GWP value, which shows the importance of using more efficient solar PV panels to produce green H_2. On the other side, any progress upstream of the electrolysis system, like more efficient production processes or application of energy sources with a lower environmental footprint in the solar PV supply chain, can result in less impactful H_2.

As it is stated in Section 4.1, the main contribution to the GWP of PV-based H_2 production is caused by the production of renewable electricity. Assuming the updated scenario for single-Si panels (the second bar), 1.68 kg CO_2 eq./kg H_2 is rooted in the photovoltaic plant, in which 67% of the GHG emission is generated by PV panels. The Chinese panels are responsible for almost 1 kg CO_2 eq./kg H_2 of the overall carbon footprint of the produced H_2. Within the PV modules production, 70% of the emission is caused by the cells, in which single-Si wafer manufacturing generates 80% of the carbon footprint. Single-crystalline silicon produced via the Czochralski process embedded 0.405 kg CO_2 eq./kg H_2, which is 65% of the emission of single-Si wafer manufacturing. Solar-grade silicon obtained from the modified Siemens process is responsible for 60% of the single-crystalline silicon corresponding GWP value. It can be interesting to mention that more than 40% of the overall GWP caused by the PV panels used to power the electrolyzer is rooted in medium-voltage Chinese electricity. This point emphasizes the importance of decarbonizing the electricity of the PV panel supply chain in order to further decrease the carbon footprint of the whole process.

Figure 12 shows the GWP values of H_2 production in three Italian regions. Lombardy, Lazio, and Sicily represent the north, center, and south of Italy, respectively. The GWP values decrease from 2.51 for Lombardy to 2.02 for Lazio and then to 1.94 kg CO_2 eq./kg H_2 for Sicily. In the case of hydrogen production in the south, almost 22% lower GWP can be obtained compared to northern production sites. Starting from the northern region, the global horizontal irradiation (for the capitals of the regions based on [89]) increases from 1500 to 1600 kWh/m^2 year for the center and then 1700 kWh/m^2 year for the south. Among these three cases, the higher the insolation, the higher the annual specific yield, which means producing a certain amount of H_2 can be obtained by a smaller area covered by PV panels, which results in lowering the GWP values. Therefore, selecting the location for the PV sites can play an important role in the final GWP value.

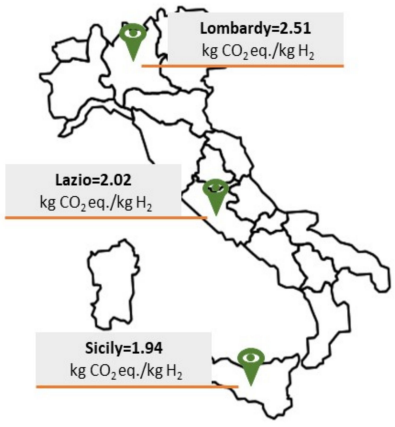

Figure 12. GWP values of each kg of H_2 for the updated scenario of single-Si PV systems for three representative Italian regions.

5. Conclusions

The literature on the life-cycle assessment of solar photovoltaic-based hydrogen production via electrolysis systems was reviewed. The background and foreground data used in the literature were identified. In the case of possibility, the type and efficiency of the modules assumed in the articles were extracted. A statistical analysis of the global warming potential values was performed. In order to compare the climate profile (carbon footprint) of H_2 production, a baseline and two updated scenarios were defined. The baseline scenario consists of the Life Cycle Inventory data published by the ecoinvent library for photovoltaic panels. The two scenarios consider the state-of-the-art modules and primary data concerning the producibility (kWh_{el}/kWp), where the photovoltaic panel supply chain, the module's efficiency, manufacturing energy, and material were revised. An alkaline electrolysis system operating in Italy was considered for all the evaluations.

The literature review showed that the average efficiency of photovoltaic modules used in the literature is around 12.95%, which is relatively low compared to the state-of-the-art. Statistical analysis of the published global warming potential values indicated that H_2 produced in Europe has a mean equal to 4.83 kg CO_2 eq./kg H_2, higher than 3.82 kg CO_2 eq./kg H_2 calculated for the rest of the world. The case study analyzed in this article shows that by updating the Life Cycle Inventory using the recent report from the International Energy Agency, the global warming potential values for single and multi-silicon photovoltaic-based H_2 decrease from 4.28 and 3.87 to 1.75 and 1.83 kg CO_2 eq./kg H_2, respectively. Using real data for electricity production per kWp (collected by Terna, the Italian electricity transmission operator), the outcomes are equal to 2.15 and 2.25 kg CO_2 eq./kg H_2, respectively. Emphasizing the findings, these revised outcomes (global warming potential values), through the updated scenarios, decrease the climate profile by 59% and 52% for single-Si and multi-Si photovoltaic systems, respectively. Similarly, suppose panels with higher efficiencies like 22% and 25% are adopted, representing a future possible evolution of the installed technology. In that case, the GWP will further decrease to 1.61 and 1.44 kg CO_2 eq./kg H_2, which can be translated to a larger reduction in the climate profile.

The analysis, in accordance with the literature, shows that the photovoltaic system-related factors as the most important player in the carbon footprint of the produced H_2 via electrolyzer plant. In other words, most greenhouse gas emissions are related to renewable electricity production through the photovoltaic system. The electrolysis of water by itself, as far as the electrolyzer production and management is concerned, is responsible for only 0.07 kg CO_2 eq./kg H_2, equal to just 2–4% of the overall value. The electrolysis technology instead impacts mostly in terms of efficiency, which directly affects the quantity of electricity requested by the hydrogen production process. From this point of view, significant additional benefits may come from the reduced electricity consumption allowed by different electrolysis technologies, such as solid oxide electrolyzer cells (SOEC), which can run at a specific electrical consumption 20–30% lower than the baseline alkaline electrolysis.

The promising updated values of GWP suggest the necessity of the application of state-of-the-art PV modules for solar photovoltaic-based H_2 production projects to reduce the climate profile of this process. Moreover, a quite significant advantage is obtained by installing the system in higher irradiance regions, in the case of Italy, with Sicily featuring a 23% lower global warming potential impact with respect to Lombardy.

The findings also prove that further advancement in the photovoltaic industry, like the development of more efficient panel manufacturing routes, in addition to using renewable electricity during the production stages, can further decrease the climate footprint and, in general, improve the environmental profile of PV-based H_2.

Supplementary Materials: The following supporting information can be downloaded at: https://www.mdpi.com/article/10.3390/en16135190/s1.

Author Contributions: Conceptualization, M.K.T., J.F., D.B. and S.C.; methodology, M.K.T., J.F. and D.B.; investigation, M.K.T. and J.F.; Supervision, D.B. and J.F.; writing—original draft preparation, M.K.T.; writing—review and editing, J.F., D.B. and S.C.; funding acquisition, D.B. and S.C. All authors have read and agreed to the published version of the manuscript.

Funding: This research was partly funded by the H2 JRP at Politecnico di Milano (https://www.fondazionepolitecnico.it/en/initiatives/hydrogen-jrp/) (accessed on 20 March 2023).

Data Availability Statement: The data presented in this study are available in the paper and in the Supplementary Material.

Conflicts of Interest: The authors declare no conflict of interest.

References

1. International Energy Agency (IEA) Hydrogen. 2022. Available online: https://www.iea.org/reports/global-hydrogen-review-2022 (accessed on 15 December 2022).
2. International Renewable Energy Agency (IRENA) Hydrogen from Renewable Power: Technology Outlook for the Energy Transition. Available online: https://www.irena.org/publications/2018/sep/hydrogen-from-renewable-power (accessed on 17 November 2022).
3. International Energy Agency (IEA) Hydrogen Projects Database. Available online: https://www.iea.org/data-and-statistics/data-product/hydrogen-projects-database (accessed on 20 November 2022).
4. EU Commission ANNEX 1 to the Commission Delegated Regulation Supplementing Regulation (EU) 2020/852 of the European Parliament and of the Council: Manufacture of Hydrogen 2021. Available online: https://eur-lex.europa.eu/legal-content/EN/TXT/PDF/?uri=CELEX:32021R2139 (accessed on 20 March 2023).
5. Bhandari, R.; Trudewind, C.A.; Zapp, P. Life Cycle Assessment of Hydrogen Production via Electrolysis—A Review. *J. Clean. Prod.* **2014**, *85*, 151–163. [CrossRef]
6. Parkinson, B.; Balcombe, P.; Speirs, J.F.; Hawkes, A.D.; Hellgardt, K. Levelized Cost of CO_2 Mitigation from Hydrogen Production Routes. *Energy Environ. Sci.* **2019**, *12*, 19–40. [CrossRef]
7. Nugent, D.; Sovacool, B.K. Assessing the Lifecycle Greenhouse Gas Emissions from Solar PV and Wind Energy: A Critical Meta-Survey. *Energy Policy* **2014**, *65*, 229–244. [CrossRef]
8. Kanz, O.; Bittkau, K.; Ding, K.; Rau, U.; Reinders, A. Review and Harmonization of the Life-Cycle Global Warming Impact of PV-Powered Hydrogen Production by Electrolysis. *Front. Electron.* **2021**, *2*, 711103. [CrossRef]
9. Wernet, G.; Bauer, C.; Steubing, B.; Reinhard, J.; Moreno-Ruiz, E.; Weidema, B. The Ecoinvent Database Version 3 (Part I): Overview and Methodology. *Int. J. Life Cycle Assess.* **2016**, *21*, 1218–1230. [CrossRef]
10. Jungbluth, N.; Stucki, M.; Frischknecht, R. *Photovoltaics, Ecoinvent Report No. 6 XII*; Swiss Centre for Life Cycle Inventories: Dübendorf, Switzerland, 2009.
11. Stolten, D.; Emonts, B. *Hydrogen Science and Engineering, 2 Volume Set: Materials, Processes, Systems, and Technology*; John Wiley & Sons: Hoboken, NJ, USA, 2016; Volume 1, ISBN 3527332383.
12. Bodner, M.; Hofer, A.; Hacker, V. H2 Generation from Alkaline Electrolyzer. *Wiley Interdiscip. Rev. Energy Environ.* **2015**, *4*, 365–381.
13. Koj, J.C.; Schreiber, A.; Zapp, P.; Marcuello, P. Life Cycle Assessment of Improved High Pressure Alkaline Electrolysis. *Energy Procedia* **2015**, *75*, 2871–2877. [CrossRef]
14. Trasatti, S. Water Electrolysis: Who First? *J. Electroanal. Chem.* **1999**, *476*, 90–91. [CrossRef]
15. Ursua, A.; Gandia, L.M.; Sanchis, P. Hydrogen Production from Water Electrolysis: Current Status and Future Trends. *Proc. IEEE* **2011**, *100*, 410–426. [CrossRef]
16. Zakaria, Z.; Kamarudin, S.K. A Review of Alkaline Solid Polymer Membrane in the Application of AEM Electrolyzer: Materials and Characterization. *Int. J. Energy Res.* **2021**, *45*, 18337–18354. [CrossRef]
17. European Union Regulation (EC) No 1907/2006 of the European Parliament and the Council of 18 December 2006. Available online: https://eur-lex.europa.eu/legal-content/EN/TXT/?uri=CELEX%3A02006R1907-20140410 (accessed on 18 November 2022).
18. Koj, J.; Wulf, C.; Schreiber, A.; Zapp, P. Site-Dependent Environmental Impacts of Industrial Hydrogen Production by Alkaline Water Electrolysis. *Energies* **2017**, *10*, 860. [CrossRef]
19. Zhao, G.; Kraglund, M.R.; Frandsen, H.L.; Wulff, A.C.; Jensen, S.H.; Chen, M.; Graves, C.R. Life Cycle Assessment of H2O Electrolysis Technologies. *Int. J. Hydrogen Energy* **2020**, *45*, 23765–23781. [CrossRef]
20. Ajanovic, A.; Sayer, M.; Haas, R. The Economics and the Environmental Benignity of Different Colors of Hydrogen. *Int. J. Hydrogen Energy* **2022**, *47*, 24136–24154. [CrossRef]
21. Bareiß, K.; de la Rua, C.; Möckl, M.; Hamacher, T. Life Cycle Assessment of Hydrogen from Proton Exchange Membrane Water Electrolysis in Future Energy Systems. *Appl. Energy* **2019**, *237*, 862–872. [CrossRef]

22. Chatenet, M.; Pollet, B.G.; Dekel, D.R.; Dionigi, F.; Deseure, J.; Millet, P.; Braatz, R.D.; Bazant, M.Z.; Eikerling, M.; Staffell, I.; et al. Water Electrolysis: From Textbook Knowledge to the Latest Scientific Strategies and Industrial Developments. *Chem. Soc. Rev.* **2022**, *51*, 4583–4762. [CrossRef]
23. Carmo, M.; Fritz, D.L.; Mergel, J.; Stolten, D. A Comprehensive Review on PEM Water Electrolysis. *Int. J. Hydrogen Energy* **2013**, *38*, 4901–4934. [CrossRef]
24. Lædre, S.; Kongstein, O.E.; Oedegaard, A.; Karoliussen, H.; Seland, F. Materials for Proton Exchange Membrane Water Electrolyzer Bipolar Plates. *Int. J. Hydrogen Energy* **2017**, *42*, 2713–2723. [CrossRef]
25. El-Emam, R.S.; Özcan, H. Comprehensive Review on the Techno-Economics of Sustainable Large-Scale Clean Hydrogen Production. *J. Clean. Prod.* **2019**, *220*, 593–609. [CrossRef]
26. Aricò, A.S.; Siracusano, S.; Briguglio, N.; Baglio, V.; Di Blasi, A.; Antonucci, V. Polymer Electrolyte Membrane Water Electrolysis: Status of Technologies and Potential Applications in Combination with Renewable Power Sources. *J. Appl. Electrochem.* **2013**, *43*, 107–118. [CrossRef]
27. Leah, R.T.; Bone, A.; Selcuk, A.; Rahman, M.; Clare, A.; Lankin, M.; Felix, F.; Mukerjee, S.; Selby, M. Latest Results and Commercialization of the Ceres Power SteelCell® Technology Platform. *ECS Trans.* **2019**, *91*, 51–61. [CrossRef]
28. Sapountzi, F.M.; Gracia, J.M.; Weststrate, C.J.; Fredriksson, H.O.A.; Niemantsverdriet, J.W. Electrocatalysts for the Generation of Hydrogen, Oxygen and Synthesis Gas. *Prog. Energy Combust. Sci.* **2017**, *58*, 1–35. [CrossRef]
29. Posdziech, O.; Schwarze, K.; Brabandt, J. Efficient Hydrogen Production for Industry and Electricity Storage via High-Temperature Electrolysis. *Int. J. Hydrogen Energy* **2019**, *44*, 19089–19101. [CrossRef]
30. Vincent, I.; Bessarabov, D. Low Cost Hydrogen Production by Anion Exchange Membrane Electrolysis: A Review. *Renew. Sustain. Energy Rev.* **2018**, *81*, 1690–1704. [CrossRef]
31. Miller, H.A.; Bouzek, K.; Hnat, J.; Loos, S.; Bernäcker, C.I.; Weißgärber, T.; Röntzsch, L.; Meier-Haack, J. Green Hydrogen from Anion Exchange Membrane Water Electrolysis: A Review of Recent Developments in Critical Materials and Operating Conditions. *Sustain. Energy Fuels* **2020**, *4*, 2114–2133. [CrossRef]
32. Raja Sulaiman, R.R.; Wong, W.Y.; Loh, K.S. Recent Developments on Transition metal–Based Electrocatalysts for Application in Anion Exchange Membrane Water Electrolysis. *Int. J. Energy Res.* **2022**, *46*, 2241–2276. [CrossRef]
33. Barbón, A.; Bayón-Cueli, C.; Bayón, L.; Carreira-Fontao, V. A Methodology for an Optimal Design of Ground-Mounted Photovoltaic Power Plants. *Appl. Energy* **2022**, *314*, 118881. [CrossRef]
34. Wong, J.H.; Royapoor, M.; Chan, C.W. Review of Life Cycle Analyses and Embodied Energy Requirements of Single-Crystalline and Multi-Crystalline Silicon Photovoltaic Systems. *Renew. Sustain. Energy Rev.* **2016**, *58*, 608–618. [CrossRef]
35. Yang, D.; Liu, J.; Yang, J.; Ding, N. Life-Cycle Assessment of China's Multi-Crystalline Silicon Photovoltaic Modules Considering International Trade. *J. Clean. Prod.* **2015**, *94*, 35–45. [CrossRef]
36. Mehedi, T.H.; Gemechu, E.; Kumar, A. Life Cycle Greenhouse Gas Emissions and Energy Footprints of Utility-Scale Solar Energy Systems. *Appl. Energy* **2022**, *314*, 118918. [CrossRef]
37. Ludin, N.A.; Mustafa, N.I.; Hanafiah, M.M.; Ibrahim, M.A.; Asri Mat Teridi, M.; Sepeai, S.; Zaharim, A.; Sopian, K. Prospects of Life Cycle Assessment of Renewable Energy from Solar Photovoltaic Technologies: A Review. *Renew. Sustain. Energy Rev.* **2018**, *96*, 11–28. [CrossRef]
38. IEA. Solar PV Global Supply Chains. Available online: https://www.iea.org/reports/solar-pv-global-supply-chains (accessed on 12 February 2023).
39. International Organization for Standardization ISO 14040:2006, Environmental Management—Life Cycle Assessment—Principles and Framework. Available online: https://www.iso.org/standard/37456.html (accessed on 5 July 2022).
40. International Organization for Standardization ISO 14044:2006, Environmental Management—Life Cycle Assessment—Requirements and Guidelines. Available online: https://www.iso.org/standard/38498.html (accessed on 5 July 2022).
41. UNEP. *Global Guidance Principles for Life Cycle Assessment Database*; UNEP DTIE Sustainable, Consumption and Production Branch: Paris, France, 2011.
42. Kakoulaki, G.; Kougias, I.; Taylor, N.; Dolci, F.; Moya, J.; Jäger-Waldau, A. Green Hydrogen in Europe—A Regional Assessment: Substituting Existing Production with Electrolysis Powered by Renewables. *Energy Convers. Manag.* **2021**, *228*, 113649. [CrossRef]
43. Pr'e Consultants B.V. SimaPro, The World's Leading LCA Software. Available online: https://simapro.com/ (accessed on 30 January 2023).
44. Ecoinvent Ecoinvent Version 3.5, Allocation, Cut-off by Classification System Model 2018. Available online: https://ecoinvent.org/ (accessed on 1 March 2023).
45. European Platform on LCA | EPLCA Developer Environmental Footprint (EF). Available online: https://eplca.jrc.ec.europa.eu/LCDN/EF_archive.xhtml (accessed on 5 February 2023).
46. Sundin, C. Environmental Assessment of Electrolyzers for Hydrogen Gas Production 2019 [Internet] [Dissertation]. 2019. Available online: http://urn.kb.se/resolve?urn=urn:nbn:se:kth:diva-260069 (accessed on 20 January 2023).
47. Valente, A.; Iribarren, D.; Dufour, J. Harmonised Life-Cycle Global Warming Impact of Renewable Hydrogen. *J. Clean. Prod.* **2017**, *149*, 762–772. [CrossRef]
48. Frischknecht, R.; Stolz, L.; Krebs, P.; de Wild-Scholten, M.; Sinha, P. Life Cycle Inventories and Life Cycle Assessments of Photovoltaic Systems, Report IEA-PVPS T12-19:2020. Available online: https://iea-pvps.org/wp-content/uploads/2020/12/IEA-PVPS-LCI-report-2020.pdf (accessed on 12 February 2023).

49. Fraunhofer Institute for Solar Energy Systems, ISE with support of PSE Projects GmbH. Photovoltaics Report. Available online: https://www.ise.fraunhofer.de/content/dam/ise/de/documents/publications/studies/Photovoltaics-Report.pdf (accessed on 5 March 2023).
50. Terna Electricity Data Archives and the Latest Electricity Report. Available online: https://www.terna.it/it/sistema-elettrico/statistiche/pubblicazioni-statistiche (accessed on 10 February 2023).
51. Trina Solar TALLMAX 415W DE15M(II). Available online: https://www.trinasolar.com/us/product/tallmax-2 (accessed on 30 January 2023).
52. IEA Solar PV Manufacturing Capacity and Production by Country and Region, 2021–2027. Available online: https://www.iea.org/data-and-statistics/charts/solar-pv-manufacturing-capacity-and-production-by-country-and-region-2021-2027 (accessed on 1 February 2023).
53. Koroneos, C. Life Cycle Assessment of Hydrogen Fuel Production Processes. *Int. J. Hydrogen Energy* **2004**, *29*, 1443–1450. [CrossRef]
54. Sko-Institut, G.K. Global Emission Model for Integrated Systems (GEMIS) Database 2002. Available online: https://www.oeko.de/service/gemis/en/ (accessed on 30 January 2023).
55. Granovskii, M.; Dincer, I.; Rosen, M. Life Cycle Assessment of Hydrogen Fuel Cell and Gasoline Vehicles. *Int. J. Hydrogen Energy* **2006**, *31*, 337–352. [CrossRef]
56. Granovskii, M.; Dincer, I.; Rosen, M.A. Exergetic Life Cycle Assessment of Hydrogen Production from Renewables. *J Power Sources* **2007**, *167*, 461–471. [CrossRef]
57. Meier, P.J. *Life-Cycle Assessment of Electricity Generation Systems and Applications for Climate Change Policy Analysis*; The University of Wisconsin-Madison: Madison, WI, USA, 2002; ISBN 0493760695.
58. Mann, M.; Spath, P. *Life Cycle Assessment of Renewable Hydrogen Production via Wind/Electrolysis: Milestone Completion Report*; National Renewable Energy Lab.: Golden, CO, USA, 2004.
59. Simons, A.; Bauer, C. Life Cycle Assessment of Hydrogen Production. In *Transition to Hydrogen*; Cambridge University Press: Cambridge, UK, 2011; pp. 13–57.
60. Ivy, J. *Summary of Electrolytic Hydrogen Production: Milestone Completion Report*; National Renewable Energy Lab.: Golden, CO, USA, 2004.
61. Jungbluth, N.; Tuchschmid, M.; de Wild-Scholten, M. Life Cycle Assessment of Photovoltaics: Update of Ecoinvent Data V2. 0. *ESU Serv. Ltd.* **2008**, *50*.
62. Lombardi, L.; Carnevale, E.; Corti, A. Life Cycle Assessment of Different Hypotheses of Hydrogen Production for Vehicle Fuel Cells Fuelling. *Int. J. Energy Environ. Eng.* **2011**, *2*, 63–78.
63. Cetinkaya, E.; Dincer, I.; Naterer, G.F. Life Cycle Assessment of Various Hydrogen Production Methods. *Int. J. Hydrogen Energy* **2012**, *37*, 2071–2080. [CrossRef]
64. Pereira, S.R.; Coelho, M.C. Life Cycle Analysis of Hydrogen—A Well-to-Wheels Analysis for Portugal. *Int. J. Hydrogen Energy* **2013**, *38*, 2029–2038. [CrossRef]
65. Argonne National Laboratory GREET Model: The Greenhouse Gases, Regulated Emissions, and Energy Use in Transportation Model. Available online: https://greet.es.anl.gov/ (accessed on 5 July 2022).
66. Reiter, G.; Lindorfer, J. Global Warming Potential of Hydrogen and Methane Production from Renewable Electricity via Power-to-Gas Technology. *Int. J. Life Cycle Assess.* **2015**, *20*, 477–489. [CrossRef]
67. PE International GaBi Software with Built-in Database (DB) Version 5. Available online: http://www.gabi-software.com (accessed on 30 January 2023).
68. Suleman, F.; Dincer, I.; Agelin-Chaab, M. Environmental Impact Assessment and Comparison of Some Hydrogen Production Options. *Int. J. Hydrogen Energy* **2015**, *40*, 6976–6987. [CrossRef]
69. Althaus, H.J.; Chudacoff, M.; Hischier, R.; Jungbluth, N.; Osses, M.; Primas, A. Life Cycle Inventories of Chemicals (Final Report Ecoinvent Data v2. 0 No. 8). *Dübendorf Switz. Swiss Cent. Life Cycle Invent.* **2007**, *8*.
70. Zhang, X.; Bauer, C.; Mutel, C.L.; Volkart, K. Life Cycle Assessment of Power-to-Gas: Approaches, System Variations and Their Environmental Implications. *Appl. Energy* **2017**, *190*, 326–338. [CrossRef]
71. Ozawa, A.; Inoue, M.; Kitagawa, N.; Muramatsu, R.; Anzai, Y.; Genchi, Y.; Kudoh, Y. Assessing Uncertainties of Well-To-Tank Greenhouse Gas Emissions from Hydrogen Supply Chains. *Sustainability* **2017**, *9*, 1101. [CrossRef]
72. National Institute of Advanced Industrial Science and Technology (AIST) IDEA (Inventory Database for Environmental Analysis). Available online: http://www.idea-lca.jp/index.html (accessed on 3 April 2023).
73. Schmidt Rivera, X.C.; Topriska, E.; Kolokotroni, M.; Azapagic, A. Environmental Sustainability of Renewable Hydrogen in Comparison with Conventional Cooking Fuels. *J. Clean. Prod.* **2018**, *196*, 863–879. [CrossRef]
74. Sadeghi, S.; Ghandehariun, S.; Rosen, M.A. Comparative Economic and Life Cycle Assessment of Solar-Based Hydrogen Production for Oil and Gas Industries. *Energy* **2020**, *208*, 118347. [CrossRef]
75. Miller, I.; Gençer, E.; Vogelbaum, H.S.; Brown, P.R.; Torkamani, S.; O'Sullivan, F.M. Parametric Modeling of Life Cycle Greenhouse Gas Emissions from Photovoltaic Power. *Appl. Energy* **2019**, *238*, 760–774. [CrossRef]
76. Al-Qahtani, A.; Parkinson, B.; Hellgardt, K.; Shah, N.; Guillen-Gosalbez, G. Uncovering the True Cost of Hydrogen Production Routes Using Life Cycle Monetisation. *Appl. Energy* **2021**, *281*, 115958. [CrossRef]

77. Colella, W.G.; James, B.D.; Moton, J.M.; Saur, G.; Ramsden, T. Techno-Economic Analysis of PEM Electrolysis for Hydrogen Production. In Proceedings of the Electrolytic Hydrogen Production Workshop, NREL, Golden, CO, USA, 27–28 February 2014.
78. Palmer, G.; Roberts, A.; Hoadley, A.; Dargaville, R.; Honnery, D. Life-Cycle Greenhouse Gas Emissions and Net Energy Assessment of Large-Scale Hydrogen Production via Electrolysis and Solar PV. *Energy Environ. Sci.* **2021**, *14*, 5113–5131. [CrossRef]
79. Hermesmann, M.; Müller, T.E. Green, Turquoise, Blue, or Grey? Environmentally Friendly Hydrogen Production in Transforming Energy Systems. *Prog. Energy Combust. Sci.* **2022**, *90*, 100996. [CrossRef]
80. Zhang, J.; Ling, B.; He, Y.; Zhu, Y.; Wang, Z. Life Cycle Assessment of Three Types of Hydrogen Production Methods Using Solar Energy. *Int. J. Hydrogen Energy* **2022**, *47*, 14158–14168. [CrossRef]
81. Kolb, S.; Müller, J.; Luna-Jaspe, N.; Karl, J. Renewable Hydrogen Imports for the German Energy Transition—A Comparative Life Cycle Assessment. *J. Clean. Prod.* **2022**, *373*, 133289. [CrossRef]
82. Freire Ordóñez, D.; Halfdanarson, T.; Ganzer, C.; Shah, N.; Dowell, N.M.; Guillén-Gosálbez, G. Evaluation of the Potential Use of E-Fuels in the European Aviation Sector: A Comprehensive Economic and Environmental Assessment Including Externalities. *Sustain. Energy Fuels* **2022**, *6*, 4749–4764. [CrossRef]
83. Aydin, M.I.; Dincer, I. A Life Cycle Impact Analysis of Various Hydrogen Production Methods for Public Transportation Sector. *Int. J. Hydrogen Energy* **2022**, *47*, 39666–39677. [CrossRef]
84. Weidner, T.; Tulus, V.; Guillén-Gosálbez, G. Environmental Sustainability Assessment of Large-Scale Hydrogen Production Using Prospective Life Cycle Analysis. *Int. J. Hydrogen Energy* **2023**, *48*, 8310–8327. [CrossRef]
85. Vilbergsson, K.V.; Dillman, K.; Emami, N.; Ásbjörnsson, E.J.; Heinonen, J.; Finger, D.C. Can Remote Green Hydrogen Production Play a Key Role in Decarbonizing Europe in the Future? A Cradle-to-Gate LCA of Hydrogen Production in Austria, Belgium, and Iceland. *Int. J. Hydrogen Energy* **2023**, *48*, 17711–17728. [CrossRef]
86. Topriska, E.; Kolokotroni, M.; Dehouche, Z.; Novieto, D.T.; Wilson, E.A. The Potential to Generate Solar Hydrogen for Cooking Applications: Case Studies of Ghana, Jamaica and Indonesia. *Renew. Energy* **2016**, *95*, 495–509. [CrossRef]
87. Hauch, A.; Küngas, R.; Blennow, P.; Hansen, A.B.; Hansen, J.B.; Mathiesen, B.V.; Mogensen, M.B. Recent Advances in Solid Oxide Cell Technology for Electrolysis. *Science* **2020**, *370*, eaba6118. [CrossRef] [PubMed]
88. Hou, G.; Sun, H.; Jiang, Z.; Pan, Z.; Wang, Y.; Zhang, X.; Zhao, Y.; Yao, Q. Life Cycle Assessment of Grid-Connected Photovoltaic Power Generation from Crystalline Silicon Solar Modules in China. *Appl. Energy* **2016**, *164*, 882–890. [CrossRef]
89. The World Bank Group GLOBAL SOLAR ATLAS. Available online: https://globalsolaratlas.info/map?c=11.523088,7.998047,3 (accessed on 28 February 2023).